Heat transfer and fluid flow characteristics of the passive method in double tube heat exchangers: A critical review

Ebrahim Tavousi [a], Noel Perera [a,*], Dominic Flynn [b], Reaz Hasan [c]

[a] School of Engineering and the Built Environment, Faculty of Computing, Engineering and the Built Environment, Birmingham City University, Birmingham, B4 7XG, UK
[b] Vehicle Efficiency, Jaguar Land Rover, Gaydon, CV35 0BJ
[c] Department of Mechanical Engineering, Military Institute of Science and Technology, Dhaka, 1216, Bangladesh

ARTICLE INFO

ABSTRACT

With the growing need for more energy, it is imperative to design efficient heat exchangers that are simpler, cheaper to manufacture, have higher heat transfer rates, and low in pressure drop. One of these heat exchangers is the double tube heat exchanger that is used in many industries. From past to present, double tube heat exchangers have caught the attention of researchers because of their simplicity and wide range of applications. This review paper contains a critical analysis of the impact of different passive methods on the heat transfer and fluid flow characteristics of the fluid in double tube heat exchangers. There are different techniques to increase the heat transfer rate in double tube heat exchangers, such as turbulator insertion, extended surface (fin), in tube geometry change, nanofluids and a combination of these techniques. All these techniques are reviewed in detail to determine the heat transfer rate and friction factor enhancement in the double tube heat exchangers. Statistical analysis was provided to compare the impacts of these different techniques on the heat transfer and fluid flow characteristics of the double tube heat exchanger performance. It was concluded that a combination of turbulator inserts and nanofluids is the best technique to increase the heat transfer rate. Also, this technique provides the highest potential for heat transfer enhancement based on the standard deviation. On the other hand, extended surface (fin) is the worst-performing technique because of the high friction factor. This review article provides new ideas and gaps in the present knowledge for further investigations.

1. Introduction

A heat exchanger is a device used to transfer thermal energy between two or more fluids, separated by solid material. The applications of heat exchangers are extensive in industries where it is used to crystallize, concentrate, distil, fractionate, pasteurize, sterilize and control a process fluid. Some common heat exchangers are cooling towers, air preheaters, evaporators, condensers, automobile radiators, and shell and tube exchangers. Heat exchangers are classified in many ways, for example, according to the transfer process, the number of fluids, surface compactness, construction, flow arrangements, and heat transfer mechanisms. One of the standard classifications is based on the construction of heat exchangers (Fig. 1). These classifications are divided into four subcategories: tubular, plate-type, extended surface, and regenerative. The tubular section is divided into four subcategories: double-pipe, shell and tube, spiral tube, and pipe coil [1, 2].

One of the common heat exchangers is the double tube heat exchanger (DTHE). These are used widely in industries and engineering applications such as refrigeration, air-conditioning, power plant, solar water heater and the process industry [3]. The main advantages of DTHEs are working with high pressure and temperature of working fluids, simple maintenance, modular construction, cost-effectiveness, and its simplicity (consisting of two concentric tubes) [4]. The purpose of using DTHEs is to transfer heat between the cold and hot regions (Fig. 2). The flow directions of hot and cold fluids in DTHEs can either be parallel or counter. It is crucial and challenging for researchers to find ways and solutions to increase the DTHE's heat transfer rate and efficiency. In this regard, extensive research carried out experimentally and numerically related to DTHEs to enhance heat transfer and improve fluid characteristics.

One of the earliest publications related to DTHEs dates back to 1928 [5]. The research into DTHEs expanded rapidly after 1928 and was divided into different categories. Some scholars focused on geometry change and the insertion of elements in inner and outer tubes [6, 7].

---

* Corresponding author.
E-mail address: Noel.Perera@bcu.ac.uk (N. Perera).

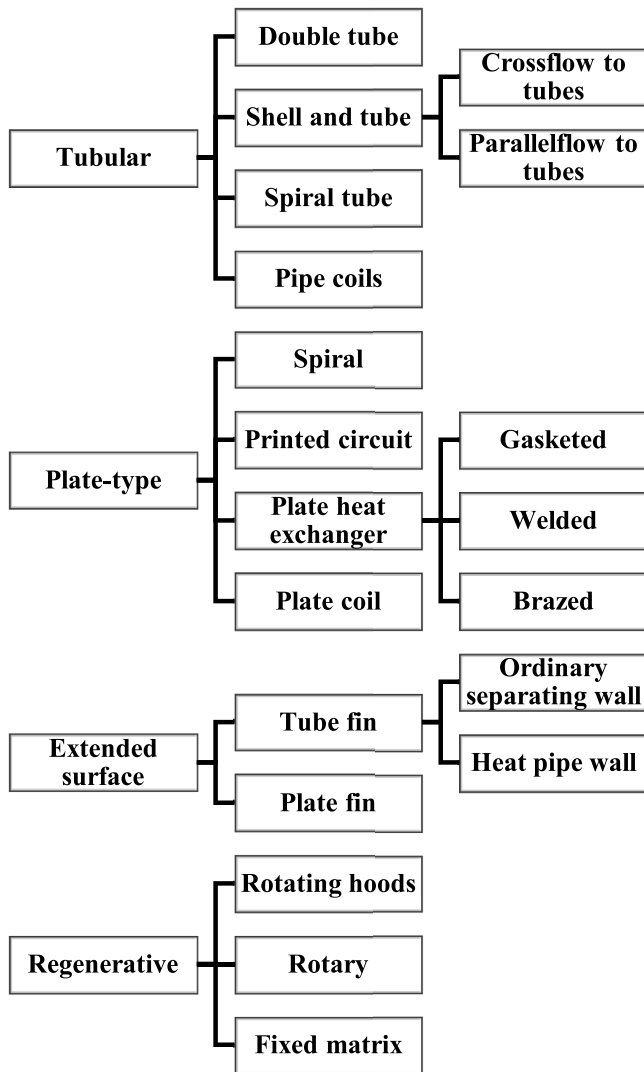**Fig. 1.** Classification of heat exchangers according to construction.

Fig. 2. Counterflow double tube heat exchanger.

$$\eta = \frac{Nu/Nu_0}{(f/f_0)^{1/3}} \tag{1}$$

Where Nu, f, Nu_0, and f_0 are the Nusselt number and friction factor for a tube with and without insert configuration, respectively.

The Nusselt number is an important measure of the convective heat transfer that can contribute to a better heat transfer rate. This parameter is expressed as:

$$Nu = \frac{hd}{k} \tag{2}$$

Where h is the convective heat transfer coefficient, d is the diameter of the tube, and k is the thermal conductivity.

Measurement of pumping power is defined as friction factor. The friction factor for a tube can be expressed as:

$$f = \frac{\Delta P}{(\rho u^2)(L/d_H)} \tag{3}$$

Where ΔP is the pressure change across the test section, ρ is the fluid density, d_H is the hydraulic diameter of the tube, u is the velocity of the fluid, and L is the length of the tube [13].

3. Heat transfer enhancement methods in DTHE

Enhancing the heat transfer rate in DTHEs is divided into three main methods: active, passive, and compound. In the active method, some external forces and energy are used to improve the heat transfer rate in the heat exchangers. For example, establishing a magnetic field for flow disturbance, using flow or surface vibration, rotating tubes and reciprocating plungers, pulsation by cams, and mechanical aids [14–18]. This method has limited practical applications because it needs extra equipment and instruments to add energy. The potential of the active method is less than the passive method as it is difficult to exert external energy in most cases [19].

In the passive methods of increasing heat transfer rate, external forces are not used to enhance the heat transfer rate in DTHEs. Some

Other researchers investigated different shapes of fins, and others investigated different working fluids such as nanofluids [8, 9]. Using external forces such as magnetic field and vibration was the interest of some scholars in the subsequent years[10–12].

This paper aims to provide a comprehensive review of the effects of the passive method such as turbulator insertion, nanofluids, geometry change, and different fin shapes on the heat transfer and performance of DTHEs.

2. Important definitions

2.1. Thermal performance factor

The thermal performance factor, η, is used to evaluate the performance of different techniques such as inserting turbulator, extended surface (fin), geometry change, using nanofluids in heat exchangers. It is a function of the heat transfer coefficient, Reynolds number and friction factor. For a particular fluid flow condition, if a method increases the heat transfer coefficient significantly with a minimum increase in the friction factor, it will produce a high thermal performance factor. The thermal performance factor is expressed as:
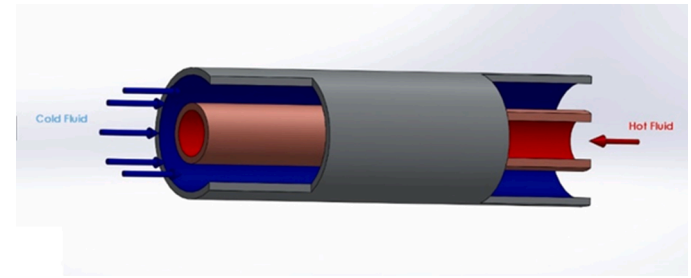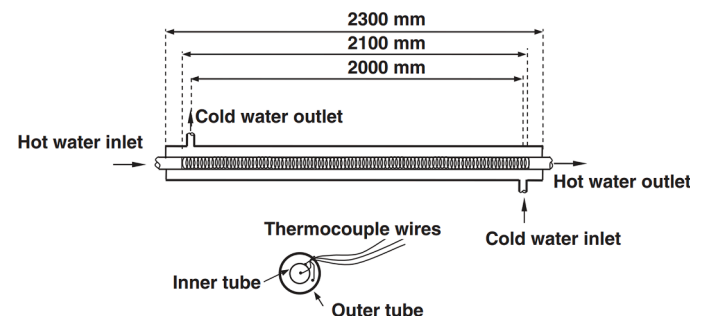

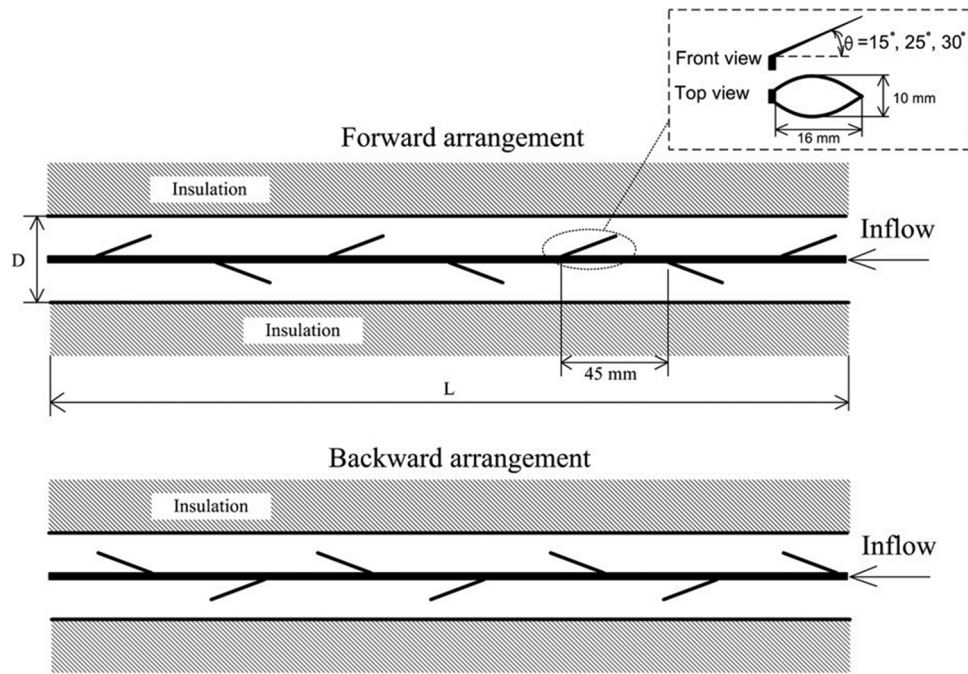**Fig. 3.** A schematic diagram of the test section [46].

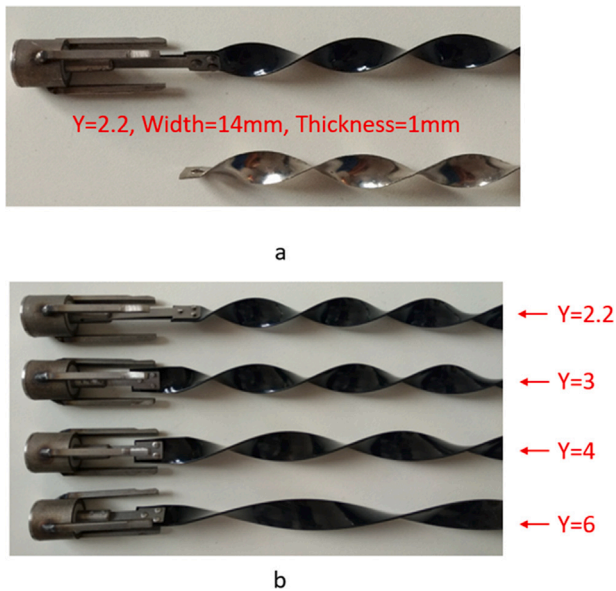**Fig. 4.** Louvered strips with forward and backward arrangements [47].

Fig. 5. (a) self-rotating twisted tapes and stationary twisted tape with the same geometry; (b) Pictorial view of self-rotating twisted tapes with different twist ratios [48].

examples of passive methods to create turbulence in the flow field are inserting fins, coiled wires, swirl flow inducement, and wall roughness. In general, the passive method is preferred compared to the active method because, in this method, there is no need for external forces and its cost-effectiveness [20, 21].

Using two or more methods of the passive and active method together to increase the heat transfer rate and performance of heat exchangers is known as the compound method [22–26]. Using various enhancement methods together increases the heat transfer coefficient in heat exchangers because of interactions among methods compared to just using one method. This compound method takes advantage of both

the external forces and induces turbulence in the flow to increase the heat transfer rate [27].

3.1. Passive method

In the passive method, there is no external forces and energy for increasing the heat transfer. Researchers find the passive method widely attractive because of the cost-effective manufacturing, no external forces, simple to set up, and low maintenance requirements. It should be mentioned that the detrimental effect of the passive methods is the increased pumping power due to the increase of the friction factor. Generally, passive methods are proposed to attain a high heat transfer rate with the smallest energy input for pumping fluids [4, 28]. Therefore, many studies have been conducted experimentally and numerically focused on this method to increase heat transfer. Some of the main techniques are turbulator insertion, extended surface area (fins), geometry changes, and using nanofluids.

In this paper, passive methods are divided into insertion elements as turbulator insertion, using different shapes of fins as extended surface area and modification in tubes and tube's wall (different roughness) as geometry change, and using nanofluids. With the passive method, the key factors that decrease the thermal boundary layer are creating secondary flow, disturbance, turbulence, and increasing the surface area.

- Turbulator insertion

Turbulator insertions are used to induce disturbance and perturbation in the flow. This is achieved by inserting the coiled wire, twisted tape, and louvered strip.
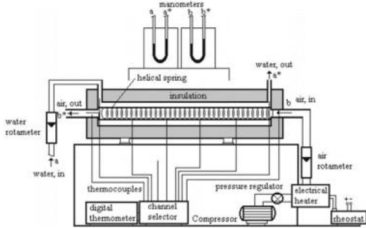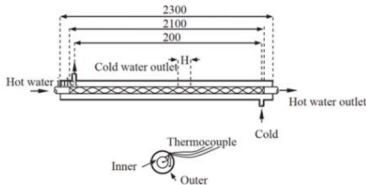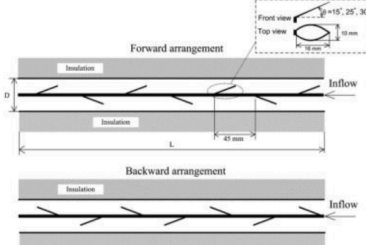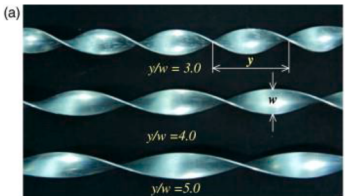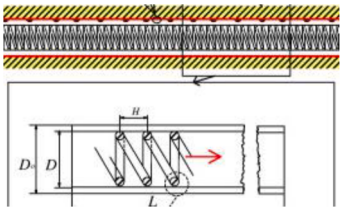
- Extended surface area (fins)

Fins are used to increase surface area, creating secondary flow and turbulence in the flow.
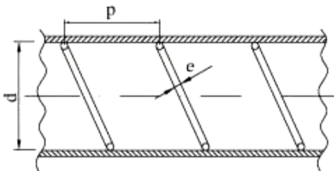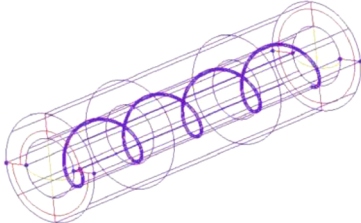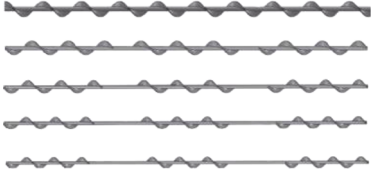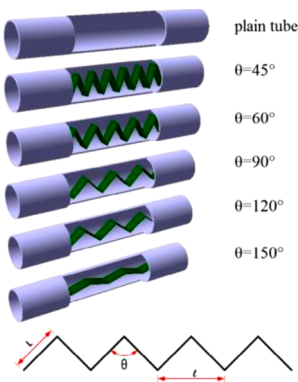
- Geometry change

Changing tubes' cross-sections, different shapes of tube walls, and

Table 1
Summary of information on different turbulators insertion compared to a conventional DTHE.

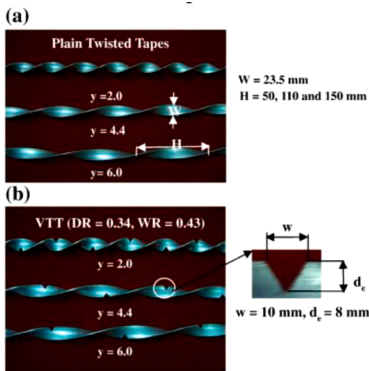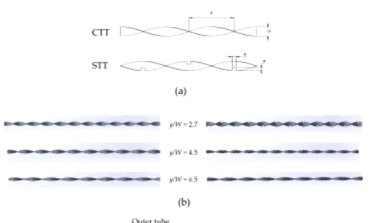| Author	Configuration	Conditions	Findings
Akpinar [51]	Helical wire	Experimental *Re*: 6500–13,000 Inner: hot air Outer: cold water Parallel and Counter flow	ü Increase of Nusselt number: 164% ü Increase of friction factor: 174%
Naphon [6]	Twisted tape	Experimental *Re*: 7000–23,000 Inner: hot water, temperature: 40–45 °C Outer: cold water, temperature: 15–20 °C Counter flow	ü Increase of heat transfer rate coefficient: up to 253% ü The overall heat transfer coefficient decreases by increasing the Reynolds number.
Eiamsa-ard, Pethkool [47]	Louvered strip	Experimental *Re*: 6000–42,000 Inner: hot water, temperature: 25 °C Outer: cold water, temperature: 25 °C Counter flow	ü Increase of average Nusselt number: 284% ü Increase of friction factor: 413%
Yadav [52]	Half-length twisted tape inserted in U-bend [53]	Experimental Inner: hot oil Outer: cold water, temperature: 25 °C Counter flow	ü Increase of heat transfer: 40% ü Thermal performance of smooth tube is better than half-length twisted tape by 30% ü Thermal performance of plain heat exchanger is better than half-length twisted tape by 30 to 50%
Shashank and Taji [54]	Coil wire with different materials (copper, aluminum, and stainless steel) [42]	Experimental *Re*: 4000–13,000 Inner: hot water Outer: cold water Counter flow	ü The increase of heat transfer for copper, aluminum, and stainless steel: 58, 41, and 31% ü The increase of friction factor for aluminum, stainless steel and copper: 570, 490, and 440% ü The friction factor increases with decreasing coil wire pitch
Sheikholeslami, Hatami [55]	Agitator	Experimental *Re*: 6000–12,000 Inner: hot water, temperature: 70, 80, 90 °C Outer: cold air Counter flow	ü Inserting the agitator in the inner tube increases the heat transfer rate ü Enhancement of heat transfer decreases with increase of Reynolds number
Moya-Rico, Molina [56]		Experimental *Re*: 6000–12,000	ü Increase of heat transfer: up to 80% ü Increase of pressure drop: up to 50%

(*continued on next page*)

Table 1 (*continued*)

Author	Configuration	Conditions	Findings
	Twisted tape	Inner: hot sugar-water mix, temperature: 57, 46, 32, and 17 °C Outer: cold propylene glycol, temperature: constant inlet 8 °C Counter flow	ü Nusselt number and friction factor is higher in the shorter spacer
Slaiman and Znad [57]	Wire coil [58]	Experimental *Re*: 5000–40,000 Inner: hot water, temperature: 60 and 70 Outer: cold water Counter flow	ü Increase of heat transfer: up to 143% ü Increase of pressure drop: up to 375% ü Maximum Nusselt number enhancement occurred at *Re*: 5000 ü Heat transfer enhancement is more effective at low values of Reynolds number than high values
Padmanabhan, Reddy [59]	Helical wire insertion	Numerical Inner: cold water, temperature: inlet 28 °C Outer: hot water, temperature: inlet 90 °C Counter flow	ü Increase of heat transfer coefficient: up to 63.91% ü The wall thermal transmission and heat flux increase by reducing the pitch gap
Ibrahim [45]	Helical screw-tape	Experimental *Re*: 570–1310 Inner: cold water Outer: hot water Counter flow	ü Increase of Nusselt number: 115% ü Increase of friction factor: 60% ü The Nusselt number increase increases with the increase of Reynolds number and with the decrease in spacer length twist ratio
Pourahmad and Pesteei [60]	Wavy strip	Experimental *Re*: 3000–13,500 Inner: hot water, temperature: 54 °C Outer: cold water Counter flow	ü Increase of effectiveness: up to 71% ü Increase of friction factor: up to 600% ü The effectiveness increases with the increase of Reynolds number and increases with the decrease of the wavy strip angle ü The effectiveness and Number of Transfer Units (NTU) have a maximum value at the angle of 45°
Murugesan, Mayilsamy [61]		Experimental *Re*: 2000–12,000 Inner: hot water, temperature: 54 °C Outer: cold water, temperature: 30 °C Counter flow	ü Increase of Nusselt number with and without cut: 150% and 100% ü Increase of friction factor with and without cut: 470% and 280% ü The V-cut twisted tape offered a higher heat transfer rate, friction factor and thermal performance factor compared to the plain twisted tape

Table 1 (*continued*)

| Author	Configuration	Conditions	Findings
	With and without V-cut twisted tape		
Wijayanta, Kristiawan [62]	Square-cut Twisted Tape	Numerical *Re*: 8000–18,000 Inner: hot water Outer: cold Counter flow	ü Increase of Nusselt number with and without cut: 80.7% and 74.4% ü Increase of friction factor with and without cut: 230% and 200% ü The decrease of the pitch ratio leads to the increase of efficiency, Nusselt number and friction factor
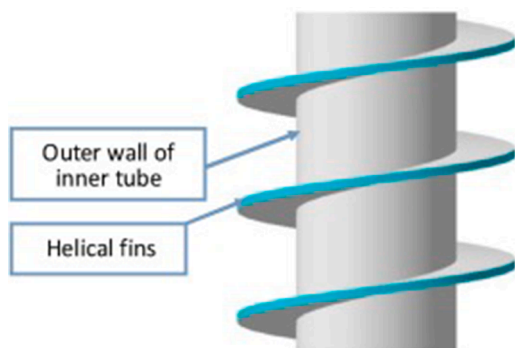
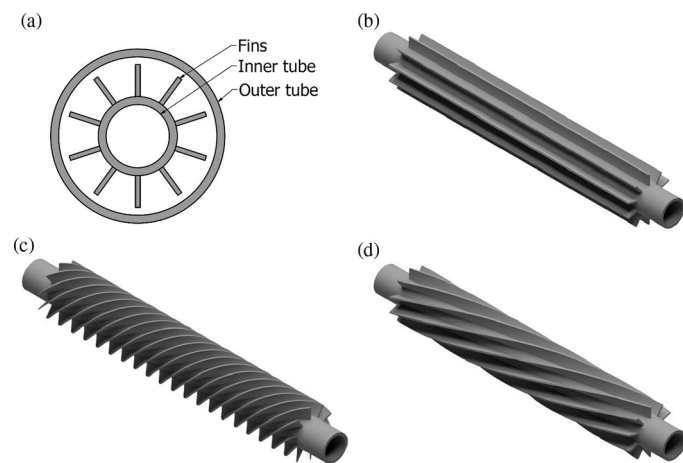**Fig. 6.** Inner tubes with helical fins and vortex generators on its outer wall [87].

Fig. 7. Models of double-pipe heat exchangers with longitudinal fins and helical fins (a) and (b) Longitudinal (c) and (d) Helical [88].
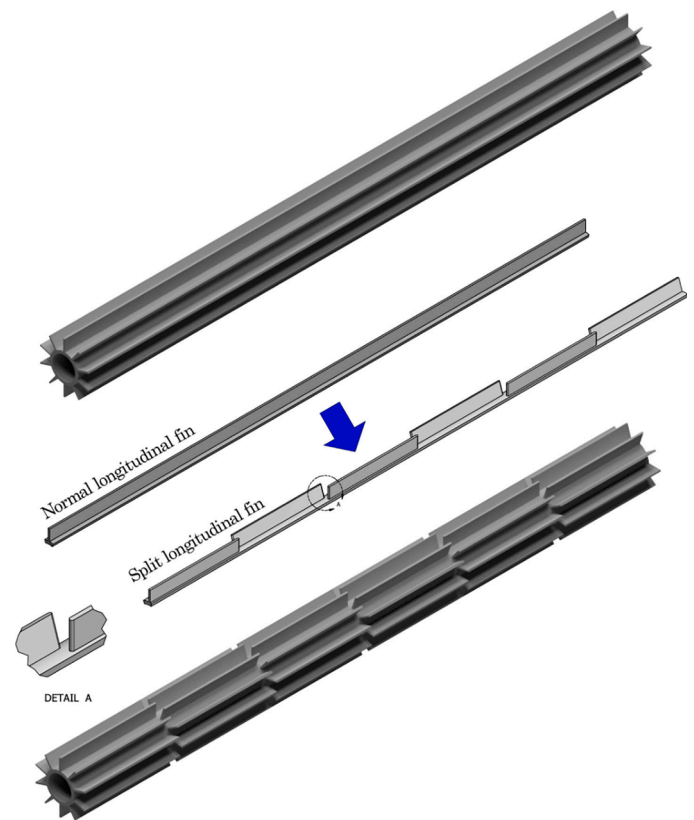

Fig. 8. Schematic of DTHEs with (a) normal longitudinal fins and (b) split longitudinal fins [89].

roughness increases the heat transfer by creating turbulence and increasing surface area. Some examples are corrugated tubes, helical tubes, and different cross-sections of tubes.

- Nanofluids

Nanofluids are used to increase heat capacity, the thermal conductivity of the base fluid, fluctuations and turbulence in the fluid flow.

- Combination of different techniques

The key factors of different techniques interact with each other in this method to increase the heat transfer rate.

4. Impact of different passive methods on the heat transfer and fluid flow characteristics of DTHE

One of the critical mechanisms to increase heat transfer between tube wall and fluid flow is reducing the thickness of the thermal boundary layer. The thickness of the thermal boundary layer is affected by the condition of fluid flow, which is smaller in the turbulent flow. Therefore, the heat transfer in the turbulent flow is faster than laminar flow because the eddies convey the thermal energy quickly in the turbulent flow and the thickness of the thermal boundary layer is smaller in the turbulent flow [28, 29]. This section discusses the impact of different passive methods on the heat transfer and fluid flow properties in a DTHE.

4.1. Turbulator insertion

Inserting turbulators are simple, easy, cost-effective, and produce a good performance in heat exchangers. Turbulator insertion increases heat transfer by mixing fluid and creating turbulence in the flow. In this way, the thermal boundary decreases, and the convective heat transfer improves [19]. There are different turbulators insertion to enhance the heat transfer in DTHEs, such as coiled wire, twisted tape, and louvered strip [30–38]. These elements are generally used in the inner tube since there is a greater heat transfer improvement [39].

There are many publications [40–44] on the effects of twisted tape, coiled wire, and louvered strip elements on the heat transfer and fluid flow properties in a DTHE. Turbulator insertion makes flows swirl and changes fluid velocity near the wall because of various vorticity distributions in the vortex core of the tube. The swirl flow induces a tangential velocity component that enhances flow mixing between the tube core and near-wall region. Although the heat transfer increased with swirl flow, the pressure drag and shear stress in the tube also increased because of the coiled wire, twisted tape, and louvered strip [45].

Naphon [6] experimentally studied typical twisted tape configuration with different pitches in a double tube heat exchanger. The working fluids were hot water for the inner tube and cold water for the outer tube. They found that inserting twisted tape increases the heat transfer coefficient and pressure drop compared to a simple double tube heat exchanger. The overall heat transfer coefficient increased by 254% and decreased by increasing the Reynolds number.

Naphon [46] experimentally studied the heat transfer characteristics and pressure drop of a DTHE with coil wire insert (Fig. 3). Cold and hot
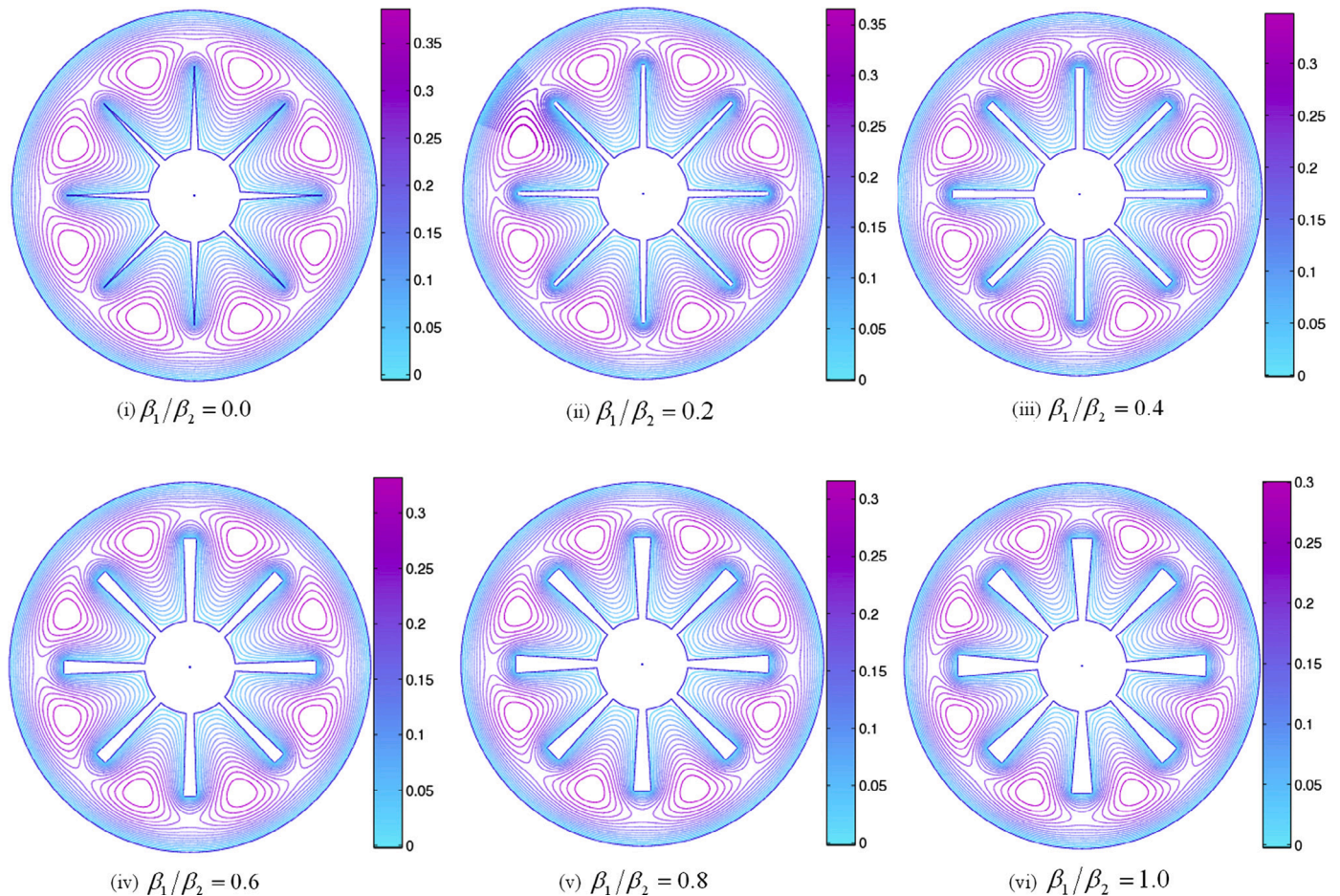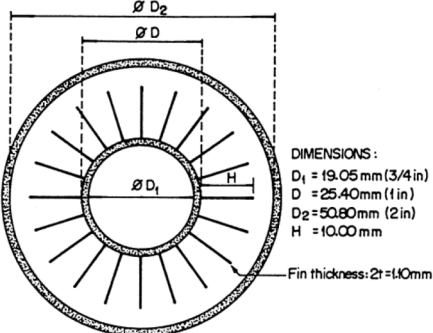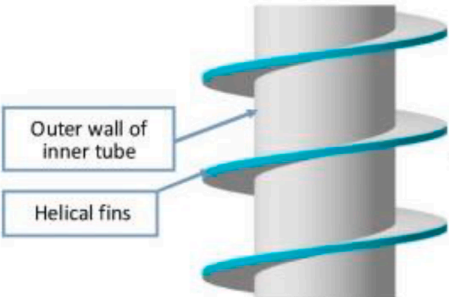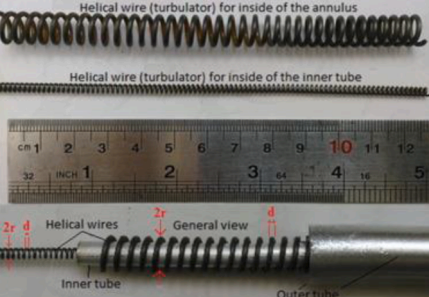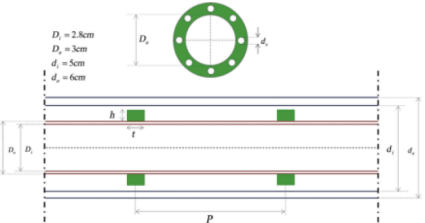
Fig. 9. Different fin-tip thickness [91].
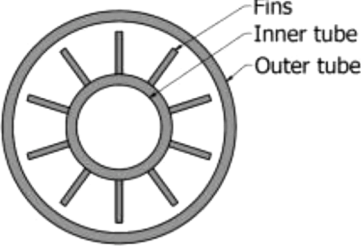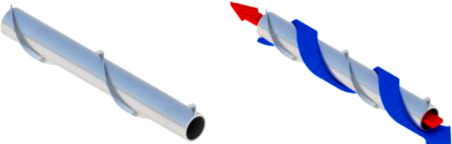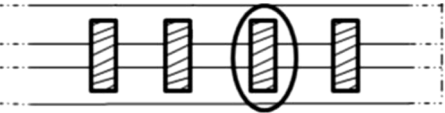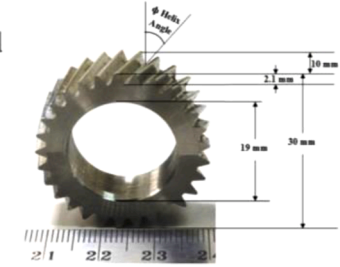
Table 2

Summary of information on different extended surface compared to a conventional DTHE.

Author	Configuration	Conditions	Findings
Braga and Saboya [8]	Longitudinal rectangular fins	Experimental and numerical *Re*: 10,000–50,000 Inner: hot water, temperature: 98 °C Outer: cold air, temperature: 10–25 °C Parallel flow	ü The fin or the region efficiency are known functions of the Reynolds number of the airflow and thermal conductivity of the fin material
Zhang, Guo [83]	Helical fins and vortex generators [87]	Experimental *Re*: 6627–13,387 Inner: steam, temperature: 100 °C Outer: cold air, temperature: 24–28 °C Counter flow	ü Increase of heat transfer: up to 46% ü Increase of pressure drop: up to 146% ü Heat exchanger with helical fins and vortex generators have better performance than heat exchangers only with helical fins at shorter pitch ratio
Zohir, Habib [92]	Coil wire around outer surface of inner tube [39]	Experimental *Re*: 4000–14,000 Inner: hot water, temperature: 65 °C Outer: cold water, temperature: 25 °C Parallel and counter flow	ü Increase of heat transfer: 450% for counterflow and 400% for parallel flow ü The Nusselt number increases with Reynolds number and pitch ratio
Sheikholeslami, Gorji-Bandpy [93]	Typical and perforated circular-ring	Experimental *Re*: 6000–12,000 Inner: hot water Outer: cold air, temperature: 28 °C Counter flow	ü Increase of Nusselt number with and without holes: 48% and 56% ü Increase of friction factor with and without holes: 310% and 650% ü Nusselt number and friction factor decrease by increasing the pitch ratio and number of perforated hole
Sheikholeslami, Gorji-Bandpy [94]	Typical and perforated discontinuous helical	Experimental *Re*: 6000–12,000 Inner: hot water Outer: cold air, temperature: 28 °C Counter flow	ü Increase of Nusselt number with and without holes: 62% and 76% ü Increase of friction factor with and without holes: 46% and 610% ü Nusselt number and friction factor decrease with the increase of pitch ratio and perforated hole
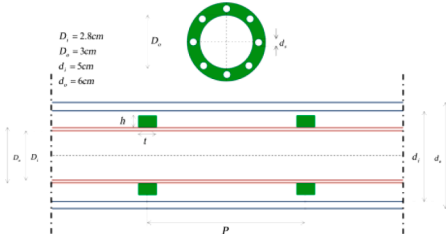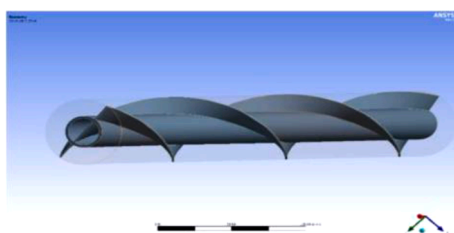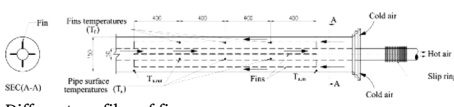
Table 2 (*continued*)

Author	Configuration	Conditions	Findings
Karanth and Murthy [95]	Rectangular, triangular and concave parabolic fin [88]	Numerical *Re*: 3000–20,000 Inner: hot water, temperature: 59 °C Outer: cold water, temperature: 30 °C Parallel flow	ü Increase of heat transfer: 128% ü Increase of pressure drop: 368% ü Rectangular fin has the highest heat transfer rate and pressure drop compared to triangular and concave parabolic fin
El Maakoul, Laknizi [96]	Continuous helical baffle	Numerical *Re*: 6000–72,000 Inner: hot water, temperature: 36–40 °C Outer: cold water, temperature: 8–17 °C Counter flow	ü Increase of heat transfer: 45% ü Increase of pressure drop: 21 times ü The highest thermo-hydraulic performance is achieved when helical baffles are used in laminar flow regime
Sreedhard and Varghese [97]	Longitudinal fin patterns [88]	Numerical *Re*: 2230 Inner: hot water, temperature: 97 °C Outer: cold water, temperature:27 °C Counter flow	ü Increase of heat transfer: 60.5% ü Maximum heat transfer and overall heat transfer coefficient is found when using four external fins
Zhang, Yu [98]	Helically petal-shaped fin	Experimental *Re*: 12,000–18,000 Inner: cold water Outer: hot water Counter flow	ü Increase of heat transfer: 233% ü Increase of pressure drop: 111% ü The increase in heat transfer is significantly greater than that of the increase in pressure drop at constant Reynolds number
Salem, Eltoukhey [99]	Helical tape	Experimental *Re*: 2050–26,700 Inner: hot water, temperature: 50 °C Outer: cold water, temperature: 15, 20, 25 °C Counter flow	ü Increase of Nusselt number: 164.4% ü Increase of friction factor: 113.1% ü The annulus average Nusselt number and friction factor increased an increase in the height ratio, and decrease in the pitch ratio
Yadav and Sahu [100]	Helical surface disk	Experimental *Re*: 3500–10,500 Inner: hot water, temperature: 75 °C Outer: cold air Counter flow	ü Increase of Nusselt number: 290% ü Increase of friction factor: 990% ü The Nusselt number increased with the increase in Reynolds number and helix angle. It decreased with an increase in the diameter ratio ü The friction factor increases with the increase in the helix angle and decreases with the increase in the diameter ratio and Reynolds number
Sheikholeslami and Ganji [101]		Experimental *Re*: 6000–12,000 Inner: hot water Outer: cold air Counter flow	ü Increase of Nusselt number: 112.5% ü Increase of friction factor: 760% ü Thermal performance enhances with augment of open area ratio ü Temperature gradient reduces with augment of the pitch ratio

Table 2 (*continued*)

Author	Configuration	Conditions	Findings
	Perforated turbulator		
Shaji [102]	Twisted Tape	Numerical *Re*: 4717–14,591 Inner: hot water, temperature: 80 °C Outer: cold water, temperature:27 °C Counter flow	ü Increase of Nusselt number: 43% ü Increase of friction factor: 177% ü Secondary flows induced by the twisted tape, enhanced cross stream mixing of the fluids, increase in the effective flow length
Yassin, Shedid [103]	Straight fin	Experimental *Re*: 30,000–90,000 Inner: hot air Outer: cold air Counter flow	ü Increase of Nusselt number: 118% ü The Nusselt number is proportional to the axial *Re*, Ta, fin heights and number of fins
Ravikumar and Raj [104]	Different profiles of fin	Numerical Mass flow: 0.01- 0.07 kg/s Inner: hot water Outer: cold water Counter flow	ü Increase of heat transfer: 220% ü Increase of pressure drop: 10%
Sivalakshmi, Raja [105]	Helical fin	Experimental Mass flow: 0.01- 0.05 kg/s Inner: hot water, temperature: 80 °C Outer: cold air, temperature: 30 °C Counter flow	ü Increase of heat transfer: 38.46% ü utilization of helical fin in water–air exchanger in annulus side could improve the heat transfer rate

water were used as a working fluid in the outer and inner sides. The results showed that heat transfer enhancement decreases by increasing Reynolds number, and wire coil insertion significantly increases the heat transfer rate in the laminar flow region.

The heat transfer rate in a DTHE can be increased by inserting louvered strips. Eiamsa-ard, Pethkool [47] experimentally investigated the louvered strips with forward, backwards, and different inclined angles (θ=15°, 25° and 30°) configuration in a DTHE (Fig. 4). It was reported that the louvered strips increased the average Nusselt number and friction loss up to 284% and 413%, respectively, compared to a conventional DTHE.

Zhang, Lu [48] conducted an experiment to study the heat transfer and fluid flow characteristics of a DTHE fitted with a stationary and self-rotating twisted tape (Fig. 5). The experiment was conducted under turbulence flow and for different twist ratios. It was observed that the self-rotating twisted tape increased the heat transfer more than the stationary twisted tape. The thermal performance factor, pressure drop, and Nusselt number also increased with decreasing twist ratios.

Other types of turbulators insertion, such as propellers and swirl generators, are used to increase the heat transfer rate. Since the increase of pressure drop of such turbulators is high compared to the increase in heat transfer rate, they are not commonly used. Yildiz, Bíçer [29] showed that using propellers as turbulators increases, the pressure drop up to 1000% with an increase of 250% in the heat transfer rate. Using swirl generators with holes in the entrance increased the Nusselt number and friction factor by 130% and 190%, respectively [49]. Aridi, Ali [50] They presented a numerical investigation on the performance of heat transfer enhancement using a trapezoidal vortex generator in a DTHE.

(a) Deformations principle

(b) Single external deformation

(c) Single internal deformation

(d) Internal and external deformations
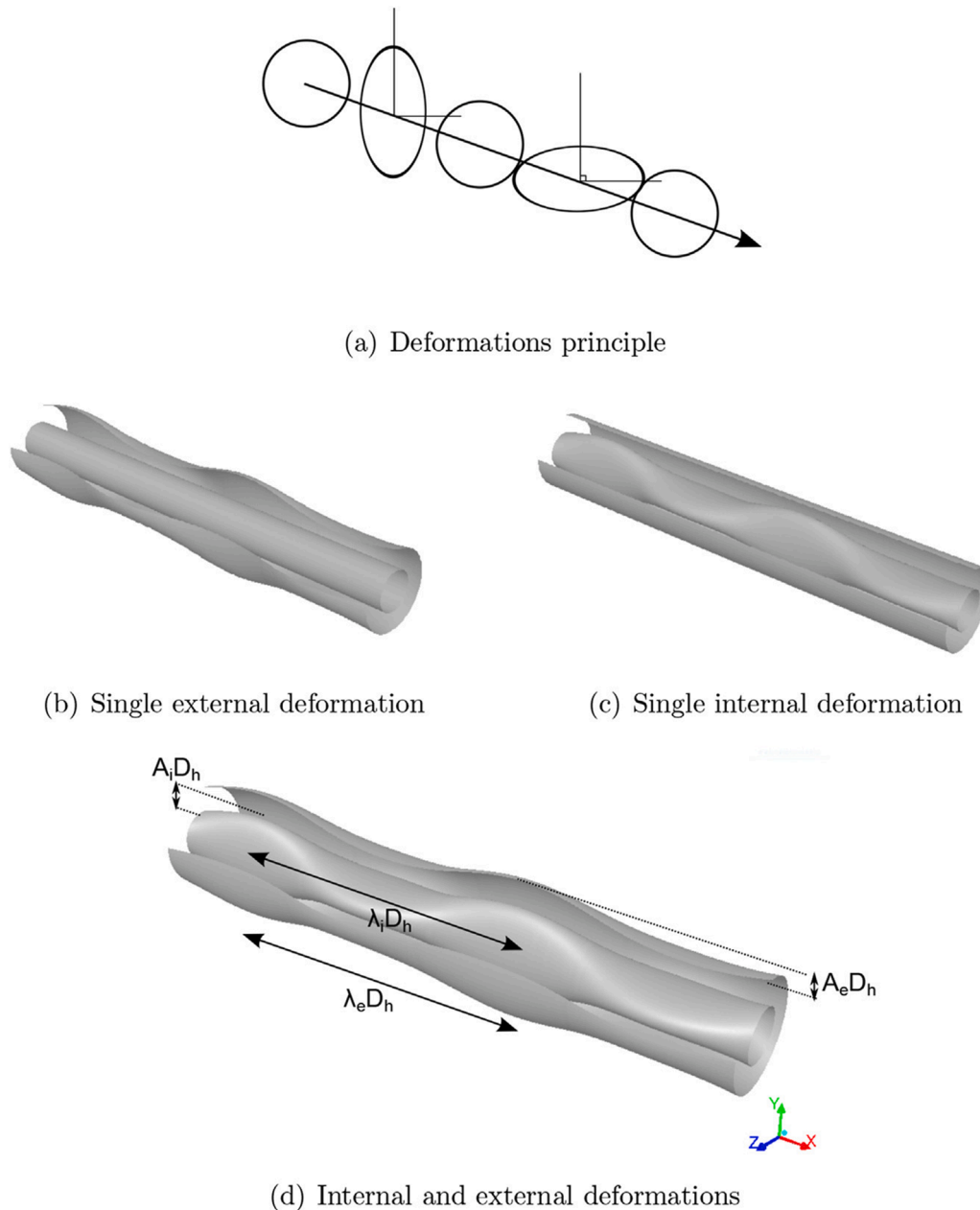
Fig. 10. Different inner and outer tube deformation [124].

They wanted two compare the effect of turbulater in three cases, including turbulator in the inner tube (case 1), in the outer side of the inner tube (case 2), and in the inner side of the outer tube (case 3). The results showed that the turbulator is effective in all cases, and the greatest improvement was 97% for case 1, 92% for case 2, and 56% for case 3. Table 1 summarises information on different turbulators insertions and their effects in comparison to a conventional DTHE.

4.2. Extended surface area (fins)

Another way to increase the heat transfer rate in DTHEs is to use fins and enlarge the surface area of fins [63–80]. This technique can help fluids with naturally low heat transfer coefficients, such as gases and high-viscosity liquids, by placing them on the fin side. Designing DTHEs by fins is very cost-effective because they are cheaper than prime tube surfaces. When fins are used in the fluid side, which has a lower heat transfer coefficient, it decreases the thermal resistance and the heat transfer capacity increases due to the bigger heat transfer surface area [81, 82]. The geometry and type of the fins are two critical factors for improving hydrothermal properties in DTHEs. These two elements establish secondary flow in DTHEs, reducing hydraulic diameter, increased surface area, vortices, and intensifying turbulence induced by the vortex generators [83–85].

In the helical fin designs, by decreasing the helical pitch, pressure drop increased sharply at a high Reynolds number; conversely, the efficiency of the heat transfer enhancement is low at the large helical pitch. So, using helical fins to enhance heat transfer is suitable for applications at low Reynolds numbers [86]. Zhang, Guo [83] installed helical fins and vortex generators on the surface of the outer tube of a DTHE and concluded that heat transfer and pressure drop increased up to 46% and 146%, respectively, compared to the conventional tube (Fig. 6).

El Maakoul, El Metoui [88] numerically studied the heat transfer and

a) Twisted square duct ($M = 10.6$)
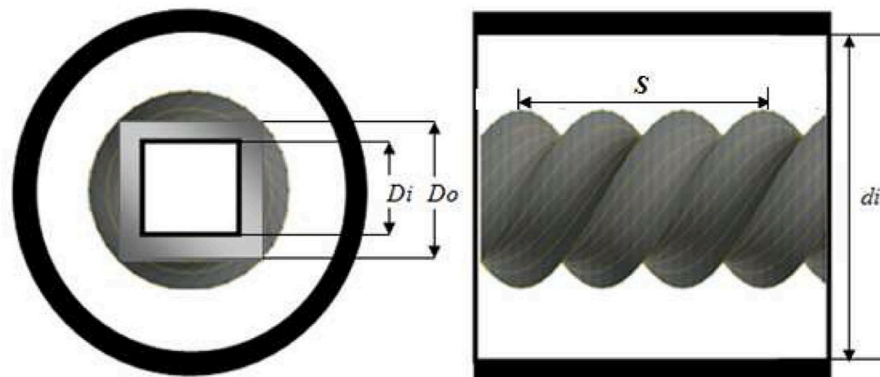
b) Terminologies for Annulus flow

$$N = \frac{di - Do}{2}$$

$$\frac{Y}{N} = 0 \quad at \; point \; o$$

$$\frac{Y}{N} = 1 \quad at \; point \; b$$
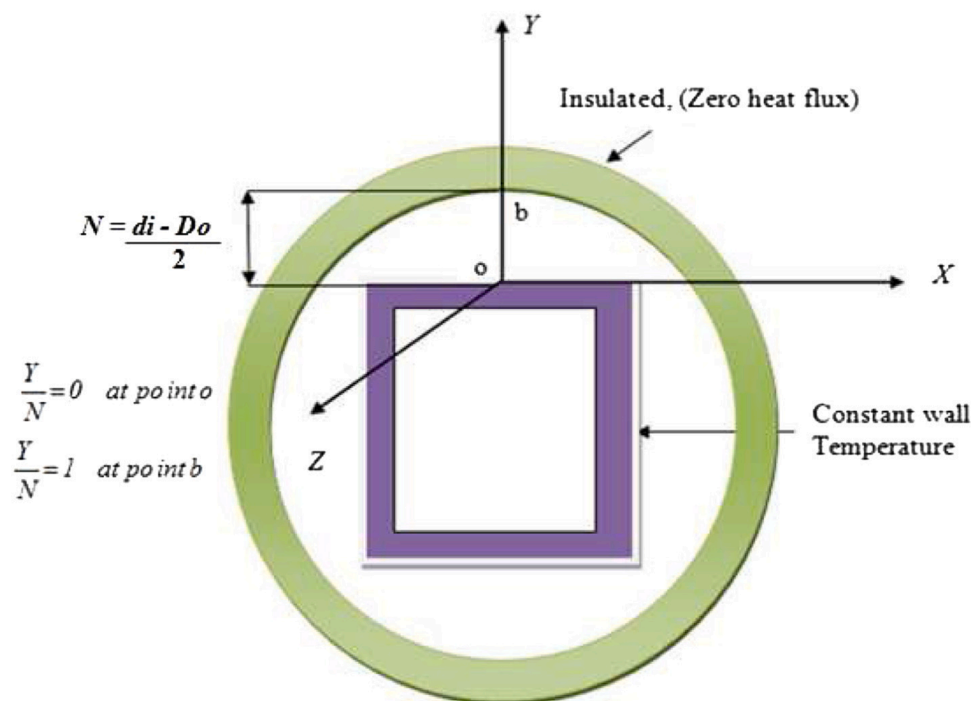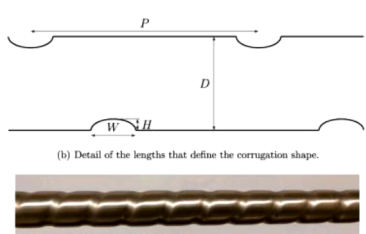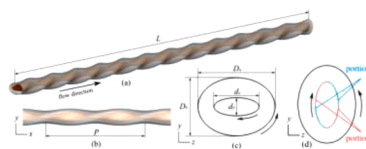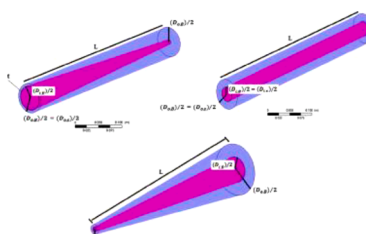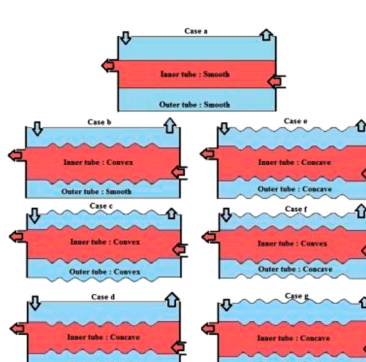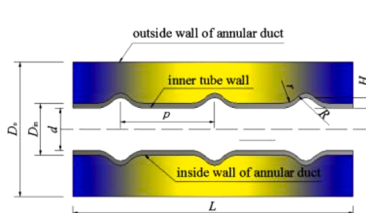
c) Boundary conditions

Fig. 11. Details of twisted square duct and outer circular pipe [128].

fluid flow characteristics and performance of an air-water DTHE with helical and longitudinal fins (Fig. 7). The results showed that helical fins have a better heat transfer rate, about 3–24% higher than longitudinal fins. It was also reported that the heat transfer rate and friction factor increased when decreasing the helical space. In another publication, El Maakoul, Feddi [89] numerically compared a DTHE with conventional longitudinal fins and split longitudinal fins (Fig. 8). The results showed that split longitudinal fins increase heat transfer 31%−48% more than conventional longitudinal fins.

Majidi, Alighardashi [90] experimentally worked on the air heat transfer in a helical fin DTHE and presented an equation for increasing the overall heat transfer coefficient due to the fin. The results showed that the presence of annulus fin increases the overall heat transfer co-efficient. Syed, Ishaq [91] introduced the tip thickness in fins design as a new parameter by significant impacts on the heat transfer and flow properties in DTHEs (Fig. 9). The tip thickness was controlled by the ratio of tip to base angles as a parameter with values varying from 0 to 1 corresponding to the fin shapes varying from the triangular to the

Table 3
Summary of information on different extended surface compared to a conventional DTHE.

Author	Configuration	Conditions	Findings
Córcoles, Moya-Rico [7]	Spirally corrugated tube (b) Detail of the lengths that define the corrugation shape.	Experimental and numerical *Re*: 25,000–50,000 Inner: cold water, temperature: 22.1 °C Outer: hot water, temperature: 60 °C Counter flow	ü Increase of average heat transfer rate: up to 23% ü Increase of pressure drop: 315 and 27% for inner and outer tube respectively ü With decreasing helical pitch and increasing corrugation height the heat transfer and pressure drop increased
Luo and Song [129]	Counter-twisted oval tubes	Numerical *Re*: 1000–15,000 Inner: wall temperature constant at 300 °C Outer: inlet temperature 20 °C Counter flow	ü Increase of Nusselt number: up to 157% ü Increase of friction factor: up to 118% ü The intensity of the vortices increases with the decrease of aspect ratio and twist ratio
Hashemian, Jafarmadar [125]	Conical tube form	Numerical *Re*: 12,202–48,808 Inner: hot water, temperature: 52 °C Outer: cold water, temperature: 25 °C Counter and parallel flow	ü Increase of Nusselt number: 63% ü Increase of friction factor: 700% ü The Nusselt number is highest in both inner and outer conical tubes
Dizaji, Jafarmadar [130]	Corrugated shell and tube	Experimental *Re*: 3500–18,000 Inner: hot water, temperature: 50 °C Outer: cold water, temperature: 22 °C Counter flow	ü Increase of NTU: 34 to 60% ü Exergy loss: 17 to 81% ü Maximum NTU is obtained for heat exchanger made of corrugated shell and corrugated tube
Han, Li [120]	Inner corrugated tube	Numerical *Re*: 26,250–65,625 Inner: constant wall temperature: 427 °C Outer: steam, temperature: 290 °C	ü Increase of Nusselt number: 81% ü Increase of friction factor: 500% ü The decrease of corrugation height and Reynolds number increase the overall heat transfer coefficient
Dizaji, Jafarmadar [119]		Experimental *Re*: 3500–18,000 Inner: hot water, temperature: 40 °C Outer: cold water, temperature: 8 °C Counter flow	ü Increase of Nusselt number: 117% ü Increase of friction factor: 254% ü Maximum effectiveness is obtained for the heat exchanger with a concave corrugated outer and convex corrugated inner tube.
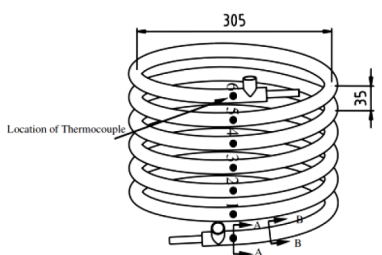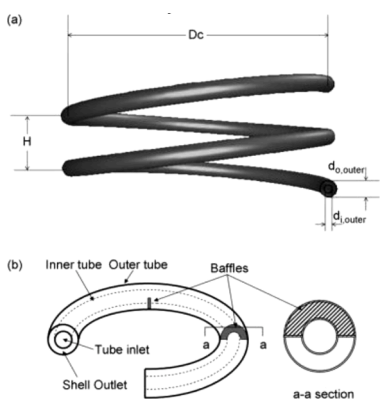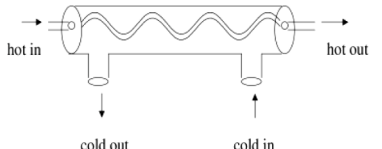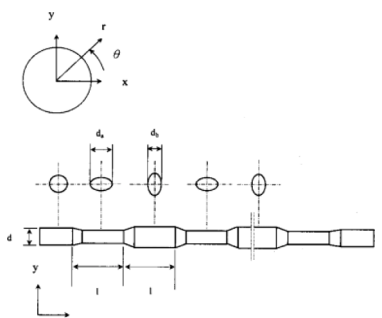
Table 3 (*continued*)

Author	Configuration	Conditions	Findings
	Convex and concave corrugated tube		
Wang, Zhang [131]	Outward helically corrugated tube	Numerical *Re*: 4300–18,800 Inner: Helium, temperature: 390 °C Outer: Helium, temperature: 300 °C Counter flow	ü Increase of heat transfer: 28% ü The heat transfer performance linearly decreased with the increase in the shell diameter, but the pressure drop sharply decreased when the shell diameter equals 38 mm
Pethkool, Eiamsa-ard [132]	Helical corrugated tube	Experimental *Re*: 5500–60,000 Inner: hot water, temperature: 70 °C Outer: cold water, temperature: 28 °C Counter flow	ü Increase of heat transfer rate: 232% ü Increase of friction factor: 115% ü The Nusselt number, friction factor and thermal performance factor increased when increasing the pitch ratio and the rib-height ratio
Laohalertdecha and Wongwises [133]	Corrugated tube	Experimental *Re*:8000–27,000 Inner: R-134a, temperature: 40, 45 and 50 °C Outer: Cold water Counter flow	ü Increase of heat transfer rate: 50% ü Increase of friction factor: 70% ü The average heat transfer coefficient and pressure drop increased when increasing the mass flux as well as average quality
Webb, Narayanamurthy [134]	Helical-rib roughness [135]	Experimental *Re*: 20,000–80,000 Inner: water Outer: R-12	ü Increase of heat transfer coefficient: 133% ü Increase of friction factor: 120% ü The area increase and fluid mixing in the interfin region caused by flow separation and reattachment are two key factors, which affect the enhancement heat transfer rate
Han, Li [136]	Outward convex corrugated tube	Numerical *Re*: 45,938–26,250 Inner: Helium, temperature: 330 °C Outer: constant wall temperature: 327 °C	ü Increase of Nusselt number: 63.6% ü Increase of friction factor: 380% ü The most significant factor in Nu is *Re*, which intensively relates to the thickness of the thermal boundary layer and turbulent intensity. ü The most significant effect factor on heat transfer and friction factor is the ratio of corrugation height to tub diameter
Wongwises and Polsongkram [137]		Experimental Mass flux: 400 and 800 kg/m².s	ü Increase of heat transfer coefficient; 33 to 53% ü Increase of pressure drop: 29 to 46%
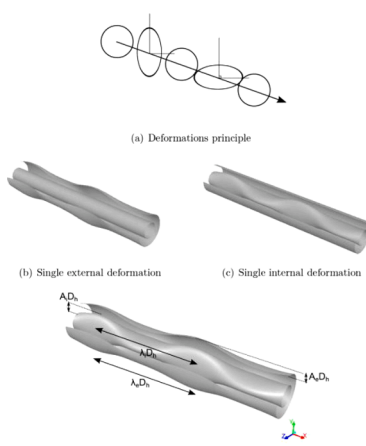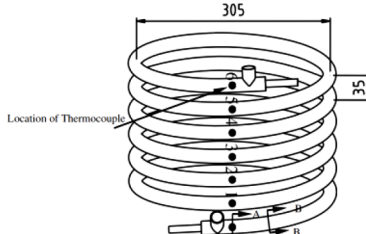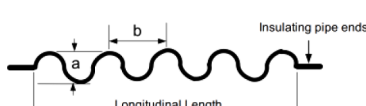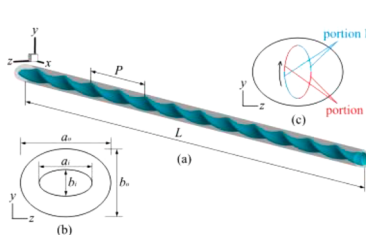
Table 3 (*continued*)

Author	Configuration	Conditions	Findings
	Helically coiled tube 	Inner: HFC-134a, temperature: 40 and 50 °C Outer: water Counter flow	ü The average heat transfer coefficient increases when increasing average vapor quality and mass flux and decreases with increasing saturation temperature ü The frictional pressure drop of the condensation process increases with increasing average vapor quality and mass flux and decreases with increasing saturation temperature of condensation
Kumar, Faizee [138]	Helically coiled tube 	Numerical *Re*: 5000–70,000 Inner: air Outer: water Counter and parallel flow	ü Increase of Nusselt number: 70% ü Increase of friction factor: 435% ü With the increase in operating pressure in the inner tube the overall heat transfer coefficient increases
Yang and Chiang [121]	Curved pipe 	Experimental *Re*: 1000–20,000 Inner: hot water Outer: cold water Counter flow	ü Increase of heat transfer rate: 100% ü Increase of friction factor: 40% ü A higher Dean number results in a higher heat transfer rate
Chen and Dung [122]	Vertical oval cross section pipe 	Numerical *Re*: 100–2000 Inner: hot water Outer: cold water Counter and parallel flow	ü Increase of heat transfer rate: 37% ü The magnitude of the overall heat transfer coefficient decreases as the total length increases, however, the heat transfer enhancement coefficient behaves oppositely, as this quantity increases while the tube is elongated
Zambaux, Harion [124]		Numerical Inner: constant wall temperature 26 °C Outer: mixture of glycol and water, temperature: 48 °C	ü Increase of heat transfer rate: 43%

Table 3 (*continued*)

Author	Configuration	Conditions	Findings
	Wall deformation		

(a) Deformations principle

(b) Single external deformation (c) Single internal deformation

(d) Internal and external deformations

Author	Configuration	Conditions	Findings
Shao, Han [139]	Helically coiled tube [137]	Experimental Mass flux: 100–400 kg/m^2.s Inner: R-134a, temperature: 35, 40 and 45 °C Outer: water Counter flow	ü Increase of heat transfer coefficient: 4 to 13.8% ü The average heat transfer coefficients for both the straight and helical sections increase with the mass flux of R-134a and the vapor quality as well

| Moawed, Ibrahim [126] | Sinusoidal inner pipe | Experimental
Re: 8800–28,000
Inner: cold water
Outer: hot water
Counter flow | ü Increase of Nusselt number: 18 to 93%
ü Increase of friction factor: 69 to 130% |

| Luo, Song [123] | Twisted oval tube | Numerical
Re: 1000–15,000
Inner: constant wall temperature 90 °C
Outer: air, temperature: 20 °C | ü Increase of Nusselt number: 116%
ü Increase of friction factor: 46%
ü The thermal performance enhancement is more significant in the laminar regime |

rectangular cross-section. Variation in fin-tip thickness appears to significantly influence the primary flow variable, the velocity field, displacing the high-velocity region and changing the velocity gradients at the wetted perimeter. Table 2 summarises information on different extended surface areas and their effects in comparison to a conventional DTHE.

4.3. Geometry change

This technique is usually used to modify the inner and outer tubes to increase the DTHEs heat transfer rate [106–116]. Corrugated tubes, helical and spiral tubes, and different cross-sections of tubes are examples of this technique that can be used widely in various industries' waste heat recovery systems [117]. This technique increases the heat transfer rate by increasing fluid mixing in the boundary layer, turbulence level of the fluid flow, and heat transfer surface area [118–120].

There are many publications that use different geometries in DTHEs to improve the heat transfer rate compared to conventional DTHEs, for example, inner curved-pipe [121], oval pipe[123, 124], coaxial annular tube with wall deformations[125], different conical tubes[126], inner sinusoidal tube[127], and inner corrugated tube[121].

Dizaji, Jafarmadar [119] performed an experiment to compare inner and outer corrugated tubes in a DTHE. It was shown that using both inner and outer corrugated tubes increased the Nusselt number and friction factor from 23–117% and 200–254%, respectively. With the inner tube being corrugated, the Nusselt number and friction factor increased from 10–52% and 150–190%, respectively. Also, Zambaux, Harion [124] numerically confirmed that the wall deformation on both inner and outer tubes increased the performance evaluation criteria up to 43% compared with only deformation on the outer or inner tube (Fig. 10).

Webb [127] showed that if the rib pitch decreased less than required
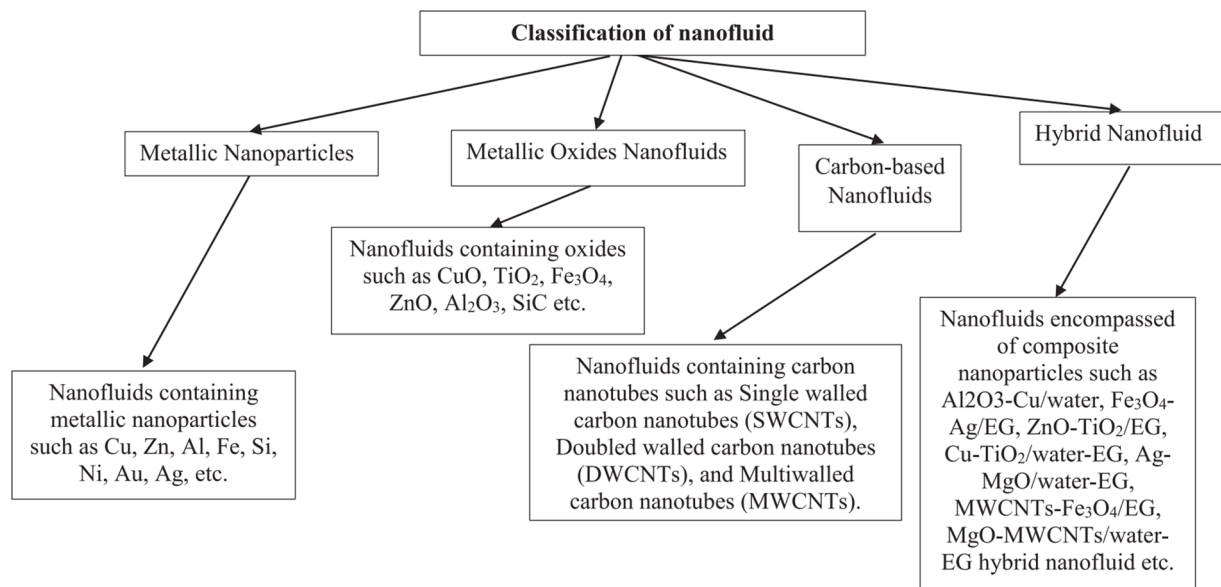
Fig. 12. Classification of nanofluid [162].

for reattachment of the boundary layer, the heat transfer coefficient decreased. So, the maximum amount occurs at the reattachment point. Bhadouriya, Agrawal [128] developed experimental and numerical investigation on hydrothermal properties in a DTHE with the inner twisted square duct and outer circular pipe (Fig. 11). It was reported that with this configuration of DTHE, the heat transfer enhancement is suitable for laminar flow rather than turbulent flow. Table 3 summarises information on different geometry changes and their effects in comparison to a conventional DTHE.

4.4. Nanofluids

Nanofluid is defined as a fluid in which nanometer-sized particles are suspended [140, 141]. Nanofluids, including suspended nanoparticles in liquids, increase the base fluids' thermal convective and conductive heat transfer performance [142]. The classification of nanofluids is various; however, they are generally classified based on nanoparticles or base fluids. The two categories of nanofluids based on nanoparticles are metallic or non-metallic nanofluids [143–145]. The suspension of metallic nanoparticles makes the metallic-based nanofluids that it can be as metal or metal oxides such as Al, Cu, Zn, CuO, ZnO [146–150]. On the other side, the non-metallic-based nanofluids are made by suspension of non-metallic nanoparticles such as SiO_2, carbon-based nanoparticles, nanofibers, graphene, graphene oxide, and nanotubes [151–155]. When more than one type of nanoparticles is used, non-metallic or metallic nanoparticles, the nanofluids are classified as hybrid nanofluids. [156–158]. According to the base fluid, nanofluids are classified as water-based, aqueous-based, or non-aqueous–based. Nanoparticles can be dispersed in different base fluids such as oils or ethylene glycol [153, 159–161]. Fig. 12 shows one of the most common classifications of nanofluids.

Nanofluids enhance the heat transfer rate by increasing the surface area of nanoparticles, heat capacity, effective and apparent thermal conductivity, interactions and collisions among particles, fluctuations and turbulence of the fluid [163, 164].

Using nanofluids in DTHEs instead of pure water or other liquids can enhance the performance of the system. So, this area of research has caught the attention of many researchers [30, 31, 165–176]. Generally, researchers investigate nanofluids as a working fluid in DTHEs. For example, some researchers investigated different nanoparticles such as

aluminum oxide, copper oxide, titanium dioxide to determine their effect on the heat transfer rate in a heat exchanger [177–179]. Table 4 summarises information on using different nanofluids and their effects in comparison to pure water in a conventional DTHE.

4.5. Combination of different techniques

To enhance the thermal performance of DTHEs, it is possible to use two or three techniques together [188, 189]. In this way, the key factors that increase the heat transfer rates reinforce each other and improve the performance of the heat exchanger. For example, a combination of turbulator insertion with geometry change [190], nanofluids with turbulator insertion and geometry change makes a good improvement in the thermal performance of DTHEs [179, 191]. Some researchers use these techniques in a single pipe with the appropriate boundary condition that matches to DTHEs to investigate the performance of DTHEs [192–209].

4.5.1. Combination of turbulator insertion and geometry change

Mashoofi, Pesteei [39] experimentally studied the thermal-frictional behavior of helically coiled a DTHE, which contains the turbulator (Fig. 13). Hot water and cold air were used as working fluids in the outer and inner tubes with inlet temperatures of 50 °C and 25 °C, respectively. The results showed that using a turbulator in the outer tube increased the airside Nusselt number by around 8–32%. However, the employment of the turbulator in the inner side increased the Nusselt number of the inner side by around 52–81%. The friction factor increased about 519% when compared to a conventional DTHE without a turbulator.

Mokkapati and Lin [190] numerically studied the combination of turbulator insertion and geometry change in a DTHE (Fig. 14). Hot water was employed in the inner corrugated tube with twisted tape insertion at 510 °C and cold water on the outer side at 90.55 °C. It showed that corrugated tubes with twisted tape insert increased the heat transfer rate by about 235.3% and 67.26% compared with a straight tube and corrugated tube without twisted tape insertion, respectively.

4.5.2. Combination of nanofluids and turbulator insertion

Chandra Sekhara Reddy and Vasudeva Rao [210] conducted experiments on TiO_2 nanofluid with the base fluid of 60% water and 40% ethylene glycol in the range of Reynolds number from 4000 to 15,000

Table 4

Summary of information on using different nanofluids in comparison to pure water in a conventional DTHE.

Author	Conditions	Findings
Chun, Kang [9]	Experimental *Re*: 100–450 Nanofluid: Al_2O_3, base fluid: water and transformer oil, concentration: 0.25% and 0.5% Inner: cold nanofluid and water Outer: hot water and nanofluid Parallel and counter flow	ü Increase of the heat transfer coefficient: up to 25% ü The surface properties of nanoparticles, particle loading, and particle shape are key factors for enhancing the heat transfer properties of nanofluids
Zamzamian, Oskouie [180]	Experimental *Re*: turbulent flow Nanofluid: Al_2O_3 and CuO, base fluid: ethylene glycol, mean diameter 20 nm, concentration: Al_2O_3: 0.1, 0.5, and 1%, CuO: 0.1, 0.3, 0.5, 0.7, and 1% Inner: hot nanofluid, temperature: 45, 60, and 75 °C Outer: cold water	ü Increase of the heat transfer coefficient: up to 37.2% ü the convective heat transfer coefficient of nanofluid increases with increasing volume fraction and temperature of nanofluid ü The theoretical and experimental results are same in lower temperatures
Darzi, Farhadi [181]	Experimental *Re*: 5000–20,000 Nanofluid: Al_2O_3, base fluid: water, mean diameter 20 nm, concentration: 0.25, 0.5, 0.75, and 1% Inner: cold nanofluid, temperature: 27–55 °C Outer: hot water	ü Increase of Nusselt number: 19% ü Increase of friction factor: 15% ü By increasing the volume fraction of nanofluid, the heat transfer and pressure drop increase ü Adding nanoparticles has better results at high Reynolds number
Aghayari, Maddah [182]	Experimental *Re*: 15,000–28,000 Nanofluid: Al_2O_3, mean diameter 20 nm, base fluid: water, concentration: 0.1, 0.2, and 0.3% Inner: hot nanofluid, temperature: 40 and 50 °C Outer: cold water Counter flow	ü The increase of heat transfer: 12% ü The nanofluid with suspended nanoparticles increases the thermal conductivity of the Mixture and a large energy exchange process resulting from the chaotic movement of nanoparticles
Sarafraz and Hormozi [183]	Experimental *Re*: 1000–11,000 Nanofluid: green tea leaves and silver nitrate, mean diameter 40–50 nm, base fluid: 50% water and 50% ethylene glycol, concentration: 0.1, 0.5 and 1%, temperature: 25–80 °C Inner: hot nanofluid Outer: cold water Counter flow	ü Increase of heat transfer coefficient: up to 67% ü Increase of friction factor: 11.3% ü Pressure drop and friction factor increases by increasing volume fraction
El-Maghlany, Hanafy [177]	Experimental *Re*: 2500–5000 Nanofluid: Cu, mean diameter: 63–100 nm, base fluid: water, concentration: 1, 1.5, 2, 2.5, and 3% Inner: hot water Outer: cold nanofluid Counter flow	ü Increase of NTU and effectiveness: 23.4% and 16.5% ü Increase of pressure drop: 36%
Han, He [178]	Experimental *Re*: 20,000–60,000 Vertical DTHE Nanofluid: Al_2O_3, base fluid: water, concentration: 0.25 and 0.5% Inner: cold nanofluid, temperature: 40 and 50 °C Outer: superheat steam Counter flow	ü Increase of Nusselt number: up to 24.5% at 50 °C ü The heat transfer increases with the increase in volume fraction and temperature of nanoparticles
Mohamed, Gutiérrez-Trashorras [184]	Numerical *Re*: 2473– 4947 Nanofluid: Al_2O_3, Cu, base fluid: water, concentration: 1, 2, and 3% Inner: hot water, temperature: 60 °C Outer: cold nanofluid, temperature: constant 28 °C Counter flow	ü Increase of average heat transfer rate: up to 13% and 7.6% for Cu and Al_2O_3 ü Increase of NTU: up to 18.8% and 10.72% for Cu and Al_2O_3 ü Increase of effectiveness: up to 13.06 and 7.56% for Cu and Al_2O_3 ü Increase of pressure drop: up to 37.26 and 27.1% for Cu and Al_2O_3 ü By increasing inlet temperature heat transfer of nanofluids increases which shows nanofluids dependency on temperature
Zheng, Wang [185]	Experimental *Re*: 4500–14,500 Nanofluid (mean diameter): Al_2O_3 (20 nm), CuO (40 nm), Fe_3O_4 (20 nm), ZnO (30 nm), SiC (40 nm), and SiO_2 (30 nm), base fluid: water, concentration: 0.5, 1, 1.5, and 2.0% Inner: cold nanofluid, temperature: 25 °C Outer: hot water, temperature: 60 °C Counter flow	ü Increase of Nusselt number (concentration): Al_2O_3: 12.2% (2%), CuO: 44.3% (1%), Fe_3O_4: 53.5% (1.5%), ZnO: 43% (1.5%), SiC: 68.4% (1.5%), SiO_2: 6.6% (0.5%) ü Increase of friction factor (concentration): Al_2O_3: 53.4% (2%), CuO: 45.5% (2%), Fe_3O_4: 73.1% (2%), ZnO: 73.5% (2%), SiC: 77.6% (2%), SiO_2: 46.4% (2%)
Esfe, Saedodin [170]	Experimental *Re*: 4000–31,000 Nanofluid: COOH-functionalized double-walled carbon nanotubes, base fluid: water, concentration: 0.01 to 0.4% Inner: cold nanofluid Outer: hot water Temperature: 300–340 K Counter flow	ü Increase of heat transfer coefficient: 32% ü Increase of pressure drop: 20% ü Nanofluid concentration of the maximum heat transfer coefficient and pressure drop: 0.4%
Duangthongsuk and Wongwises [186]	Experimental *Re*: 3000–18,000	ü Increase of heat transfer coefficient: 26% ü Increase of pressure drop: 28%

Table 4 (*continued*)

Author	Conditions	Findings
	Nanofluid: TiO_2, mean diameter: 21 nm, base fluid: water, concentration: 0.2 to 2% Inner: cold nanofluid, temperature: 15, 20, 25 °C Outer: hot water, temperature: 35, 45 °C Counter flow	ü The pressure drop of nanofluids increases with increasing Reynolds number and there is a small increase with increasing particle volume concentrations
Arani and Amani [171]	Experimental *Re*: 8000–51,000 Nanofluid: TiO_2, mean diameter: 30 nm, base fluid: water, concentration: 0.002 to 0.02 Inner: cold nanofluid Outer: hot water, temperature: 60 °C Counter flow	ü Increase of heat transfer coefficient: 72% ü Increase of pressure drop: 54% ü The use of nanofluid with the higher concentration provides considerably higher Nusselt number and thermal performance for all Reynolds numbers examined
Esfe, Saedodin [172]	Experimental *Re*: 3200–19,000 Nanofluid: MgO, mean diameter: 40 nm, base fluid: water, concentration: 0.0625 to 1% Inner: cold nanofluid, temperature: 24.7 to 60 °C Outer: hot water Counter flow	ü Increase of heat transfer coefficient: 35.93% ü Increase of pressure drop: 16% ü The maximum thermal conductivity is belonged to maximum nanofluid concentration
Khalifa and Banwan [173]	Experimental *Re*: 3000–6000 Nanofluid: Al_2O_3, mean diameter: 10 nm, base fluid: water, concentration: 0.25 to 1% Inner: cold nanofluid, temperature: 20 to 35 °C Outer: hot water, temperature: 50 °C Counter flow	ü Increase of heat transfer coefficient: 22.8% ü Increase of Nusselt number: 20% ü The heat transfer coefficient and Nusselt number are increased by increasing Reynolds number and particles volume fraction
Madhesh and Kalaiselvam [187]	Experimental *Re*: 300–700 Nanofluid: Ag, mean diameter: 10–65 nm, base fluid: ethylene glycol, concentration: 0.1 to 2% Inner: hot nanofluid, temperature: 60 °C Outer: cold water, temperature: 40 °C Counter flow	ü Increase of heat transfer coefficient: 54.3% ü Increase of pressure drop: 23.7% ü At a lower volume concentration, the mean free path available for particles moving between the inner fluids layers could benefit in transferring the heat effectively
Khedkar, Sonawane [174]	Experimental *Re*: 500–4000 Nanofluid: TiO_2, mean diameter: 20 nm, base fluid: water, concentration: 2 and 3% Inner: cold nanofluid Outer: hot water, temperature: 55–75 °C Counter flow	ü Increase of heat transfer coefficient: 33% ü For the same range of Reynold's number, addition of nanoparticles to the base fluid enhances the heat-transfer performance and results in the higher heat transfer coefficient than that of the base fluid

(Fig. 15). Nanofluid with the mean diameter of nanoparticles 21 nm and hot water flowed in the inner and outer tube as working fluids, respectively. This study aimed to indicate the effects of nanofluid with and without helical coil insertion. The results showed that heat transfer coefficient enhancement due to nanofluid with and without helical insertion was 17.71% and 10.73%, respectively. However, the friction factor increased by16.58% due to nanofluid and helical coil insertion. Table 5 summarises information on the combination of different nanofluids and turbulator insertion and their effects in comparison to pure water and a conventional DTHE.

4.5.3. Combination of nanofluids and geometry change

Qi, Luo [179] represented an experimental study to investigate a combination of corrugated tubes and nanofluid in DTHEs based on thermal efficiency assessment (Fig. 16). TiO_2–H_2O nanofluid and water were used as working fluids in outer and inner tubes, respectively. The results showed that the overall thermal performance was significantly enhanced using nanofluids and corrugated tubes, which was reflected in the increase of the Number of Transfer Units (NTU) and its effectiveness. In the best condition, the NTU was improved by 47.5%. However, for thermal fluid in the shell-side, the NTU and effectiveness decreased firstly and then increased with an increase in the Reynolds number. Table 6 summarises information on the combination of different nanofluids and geometry change and their effects in comparison to pure water and a conventional DTHE.

5. Statistical investigation

A statistical investigation was performed on 100 published articles to determine the impact of the different techniques on the heat transfer and friction factor. Twenty data were randomly selected for each technique from 1998 to 2022 to have a logical and equitable comparison among all techniques. Fig. 17 show the average heat transfer and friction factor augmentation for the combination of nanofluid and turbulator insertion, turbulator insertion, extended surface area, geometry change, and nanofluids in DTHEs. Reviewing articles in these five categories showed that the combination of nanofluid and turbulator insertion technique had the highest heat transfer enhancement of an average of 131% as compared to the other techniques. This technique employs the beneficial characteristics of turbulator insertion and nanofluids simultaneously. Hence, the properties include the increase of nanoparticles' surface area, heat capacity, effective and apparent thermal conductivity, interactions and collisions among particles from the nanofluid technique and creating effective fluid mixing, secondary flow, turbulence, swirl, and fluid velocity change near the wall in the presence of turbulator insertion make the thermal boundary layer decrease, and the heat transfer rate improves in DTHEs. The turbulator insertion technique is rated second with an average of 120% enhancement in the heat transfer rate. It showed the significance of the impact of turbulator insertion on increasing the heat transfer rate in DTHEs. The extended surface area improved the heat transfer by an average of 110% more than the geometry change and nanofluids technique. Extended surface area by establishing secondary flow, vortices, intensification of turbulence and
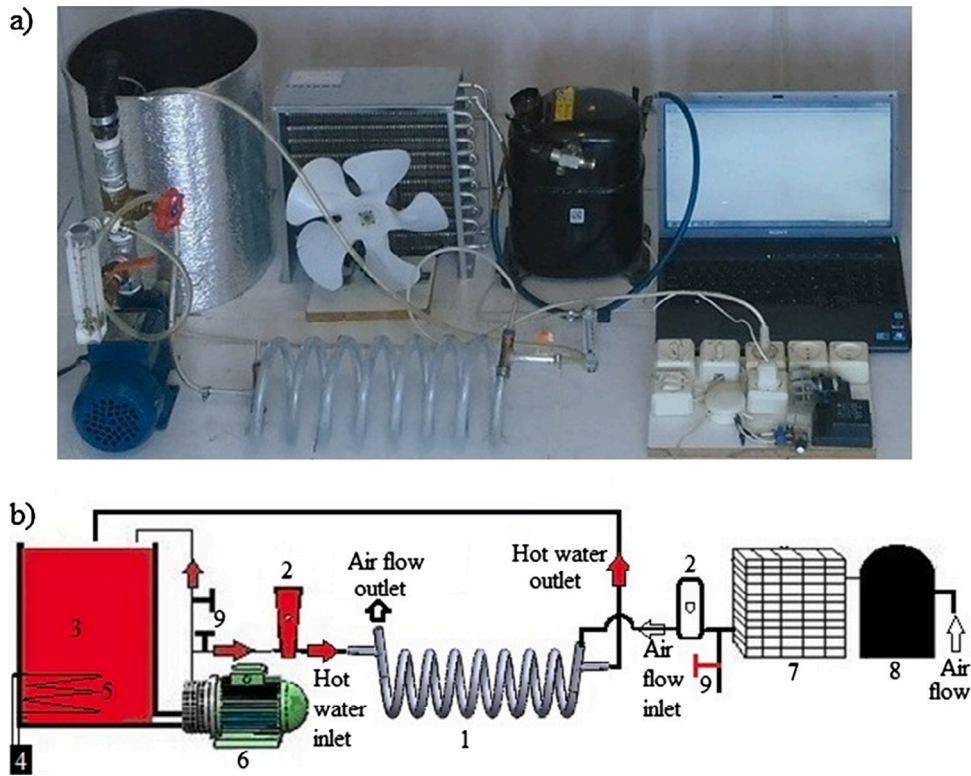
Fig. 13. (a) Experimental setup and (b) a schematic illustration of the test set-up: 1-test section, 2-Rotameter, 3-warm water tank, 4-dimmer and thermostat, 5-heater, 6-water pump, 7- condenser, 8-compressor, 9-valves [39].
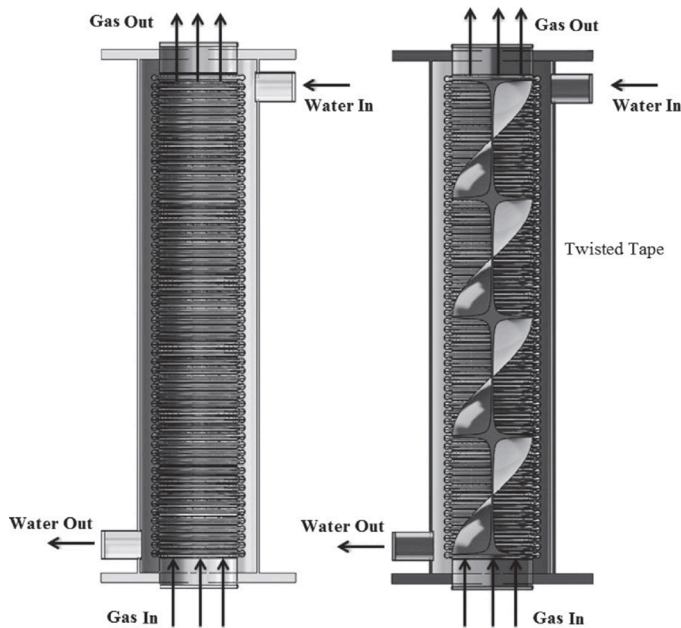
Fig. 14. Cross sectioned view of (A) ACT heat exchanger and (B) ACT heat exchanger with twisted tape [190].

Fig. 15. Photograph of wire coil inserts [210].

increasing heat transfer area in the annulus side improves heat transfer rate. In this technique, fins in the outer tube side cause turbulating in the fluid flow. However, the main thermal boundary layer for increasing the heat transfer is on the inner tube side. In addition, the concentration of fins is on the increment surface area, not turbulating and mixing fluid flow, so this technique has a lower heat transfer enhancement in

comparison to turbulator insertion. It can be concluded that creating mixing fluid flow and turbulator is more effective in the inner tube compared to the outer tube. The geometry change and the use of nanofluids have the lowest heat transfer enhancement by an average of 91% and 35%, respectively. In these techniques, creating turbulence and mixing in the fluid are not as effective as the turbulator insertion and extended surface area. It can be concluded that increasing the convective and conductive heat transfer coefficient of the base fluid are the main reasons for the heat transfer enhancement when using nanofluids. The fluctuation and turbulence of nanoparticles in the flow have a low effect on increasing the heat transfer rate compared to other techniques. Using nanofluids does not significantly improve the heat transfer rate. Hence, incorporating the use of nanofluids with other techniques is recommended.

As shown in Fig. 17, the extended surface area has the highest increment of friction factor, an average value of 536% than the other techniques This is due to the presence of the fins giving a larger surface area against the flow in comparison to the turbulator insertion, geometry change, and nanofluids techniques. The average friction factor increment of the turbulator insertion, geometry change, and

Table 5

Summary of information on the combination of different nanofluids and turbulator insertion and their effects compared to pure water and a conventional DTHE.

Author	Conditions	Findings
Maddah, Alizadeh [191]	Experimental Twisted tape *Re*: 5000–21,000 Nanofluid: Al_2O_3, mean diameter 20–22 nm, base fluid: water, concentration: 0.2, 0.5, and 0.9% Inner: hot nanofluid, temperature: constant inlet 40 °C Outer: cold water, temperature: constant inlet 25 °C Counter flow	ü Increase of heat transfer rate: up to 300% ü Increase of friction factor: up to 180%
Chandra Sekhara Reddy and Vasudeva Rao [210]	Experimental Helical coil *Re*: 4000–15,000 Nanofluid: TiO_2, mean diameter 21 nm, base fluid: 60% water and 40% ethylene glycol, concentration: 0.004, 0.012, and 0.02% Inner: cold nanofluid Outer: hot water Counter flow	ü Increase of heat transfer due to nanofluid: up to 10.73% ü Increase of heat transfer due to nanofluid and helical coil: up to 17.71% ü Increase of friction factor due to nanofluid and helical coil: up to 16.58%
Prasad, Gupta [211]	Experimental Trapezoidal-cut twisted tape *Re*: 3000–30,000 Nanofluid: Al_2O_3, mean diameter less than 50 nm, base fluid: water, concentration: 0.01 and 0.03% Inner: cold nanofluid Outer: hot water, temperature: 70 °C Counter flow	ü Increase of Nusselt number: 34.24% ü Increase of friction factor: 29% ü The average Nusselt number increase by increasing Reynolds number
Karimi, Al-Rashed [212]	Numerical Twisted tape *Re*: 250–2250 and 3000–9000 Nanofluid: Al_2O_3, base fluid: water, mean diameter 20 nm, concentration: 1, 2, and 3% Inner: cold nanofluid, temperature: 26 °C Outer: superheat steam, temperature: 37 °C Counter flow	ü Increase of the Nusselt number due to twisted tape: 22% ü Increase of heat transfer due to twisted tape and nanoparticles: up to 30% ü Increase of the pressure drop due to twisted tape and nanoparticles: up to 40% ü The use of twisted tapes at high Reynolds numbers is more economical compared to low Reynolds numbers.
Gnanavel, Saravanan [213]	Numerical Spiral Spring insertion *Re*: 1000–10,000 Nanofluid: TiO_2, BeO, ZnO, and CuO, base fluid: water Inner: hot nanofluid Outer: cold water	ü Increase of Nusselt number: TiO_2: 117.39%, BeO: 63.09%, ZnO: 56.63%, and CuO: 47.62% ü Increase of friction factor: CuO: 312%, ZnO: 304.89%, BeO: 288%, TiO_2: 275.55% ü The thermal performance factor tends to decrease with the rise of Reynolds number, for most of the cases
Karuppasamy, Saravanan [214]	Numerical Cone shape insertion *Re*: 2000–10,000 Nanofluid: Al_2O_3 and CuO, mean diameter 100 nm, base fluid: water, concentration: 1%	ü Increase of Nusselt number: Al_2O_3: 65%, CuO: 56% ü Increase of friction factor: Al_2O_3: 50%, CuO: 47% ü Aluminum oxide nano fluid gives the higher heat transfer rate than the copper Oxide nano fluid because of the nano layer and thermophysical properties of liquid and nanosolid particles
Singh and Sarkar [158]	Experimental Tapered wire coil *Re*: 9000–40,000 Nanofluid: Al_2O_3 + MgO (50/50 vol ratio), mean diameter less than 50 nm for Al_2O_3 and 90 nm for MgO, base fluid: water, concentration: 0.1% Inner: hot nanofluid, temperature: 50, 60, and 70 °C Outer: cold water, temperature: constant at 30 °C Counter flow	ü Increase of the Nusselt number: up to 84% ü Increase of the friction factor: up to 68% ü Nusselt number increases with increase in temperature from 50 to 70 °C ü The entropy generation of nanofluid is lower than the base fluid in all cases
Singh and Sarkar [215]	Experimental V-cut twisted tape *Re*: 8000–40,000 Nanofluid: Al_2O_3, PCM, and Al_2O_3+PCM, mean diameter 50 nm, base fluid: water, concentration: 0.01 and 0.1% Inner: cold nanofluid, temperature: 30 °C Outer: hot water, temperature: constant at 60 °C Counter flow	ü Increase of heat transfer coefficient due to the nanofluid: up to 25.6% ü Increase of pressure drop due to the nanofluid: up to 16.05% ü Increase of heat transfer coefficient due to the nanofluid and V-cut twisted tape: up to 47.62% ü Increase of pressure drop due to the nanofluid and V-cut twisted tape: up to 63.69%
Singh and Sarkar [216]	Experimental Conical wire coil insertion *Re*: 9000–45,000 Nanofluid: Al_2O_3, CNT, hybrid (Al_2O_3+CNT), mean diameter: 10–100 nm, base fluid: water, concentration: 0.01% Inner: cold nanofluid, temperature: 30 °C Outer: hot water, temperature: 60 °C Counter flow	ü Increase of Nusselt number (hybrid nanofluid): up to 171, 152, and 139% for diverging, converging-diverging and converging wire coil insertion ü Increase of friction factor (hybrid nanofluid): up to 106, 92, and 72% for diverging, converging-diverging and converging wire coil insertion ü The hybrid nanofluid has better heat transfer than Al_2O_3 and CNT ü CNT nanofluid has better heat transfer than Al_2O_3
Mohammed, Hasan [3]	Numerical Louvered strip insert *Re*: 10,000–50,000 Nanofluid: Al_2O_3, CuO, SiO_2 and ZnO, mean diameter 20–50 nm, base fluid: water, concentration: 1–4%	ü Increase of heat transfer: 367–411% for backward louvered strip arrangement and 350–400% for forward louvered strip arrangement ü Increase of friction factor: 900% ü SiO2 nanofluid has the highest Nusselt number value, followed by Al_2O_3, ZnO, and CuO

Table 5 (*continued*)

Author	Conditions	Findings
Sundar, Bhramara [165]	Inner: nanofluid Outer: constant heat flux Experimental Wire coil insert *Re*: 16,000–30,000 Nanofluid: Fe_3O_4, base fluid: water, concentration: 0.005–0.06% Inner: hot nanofluid, temperature: 60 °C Outer: cold water, temperature: 29 °C Counter flow	ü The Nusselt number increases with decreasing the nanoparticle diameter and it increases slightly with increasing the volume fraction of nanoparticles ü Increase of Nusselt number: 32.03% ü Increase of friction factor: 16.2% ü The heat transfer of nanofluids increases with increasing particle concentration, Reynolds number and decreasing pitch ratio of the wire coil inserts
Akyürek, Geliş [30]	Experimental Wire coil insert *Re*: 4000–20,000 Nanofluid: Al_2O_3, mean diameter less than 100 nm, base fluid: water, concentration: 0.4–1.6% Inner: cold nanofluid Outer: hot water, temperature: 70 °C Counter flow	ü Increase of Nusselt number: 271.92% ü Increase of friction factor: 500% ü The Nusselt number increase as the pitch of the turbulators placed in the heat exchanger decreases
Khoshvaght-Aliabadi, Shabanpour [217]	Experimental Perforated-tape, jagged-tape, twisted-tape, helical-screw, vortex-generator, offset-strip Flow rate: 2–5 l/min Nanofluid: Cu, mean diameter 40 nm, base fluid: water, concentration: 0.1 and 0.3% Inner: cold nanofluid, temperature: 30 °C Outer: steam Counter flow	ü Increase of Nusselt number: 293% ü Increase of pressure drop: 509% ü The vortex-generator gets the highest effect and perforated-tape gets the lowest effect
Prasad, Gupta [218]	Experimental Helical tape insert *Re*: 3000–30,000 Nanofluid: Al_2O_3, mean diameter less than 50 nm, base fluid: water, concentration: 0.01 and 0.03% Inner: cold nanofluid Outer: hot water Counter flow	ü Increase of Nusselt number: 32.91% ü Increase of friction factor: 38% ü The pressure drop in the inner tube increases with an increase in nanoparticle volume concentration and aspect ratio of the insert
Khoshvaght-Aliabadi, Akbari [219]	Experimental Vortex-generator insert *Re*: 5200–12,200 Nanofluid: Cu, base fluid: water, concentration: 0.2% Inner: cold nanofluid Outer: hot water Counter flow	ü Increase of Nusselt number: 123.9% ü Increase of pressure drop: 203.4% ü The winglets-width ratio, winglets-pitch ratio, and winglets-length ratio have strong effects on the heat transfer and pressure drop
Prasad and Gupta [220]	Experimental Twisted tape insert *Re*: 3000–30,000 Nanofluid: Al_2O_3, mean diameter less than 50 nm, base fluid: water, concentration: 0.01 and 0.03% Inner: cold nanofluid Outer: hot water Counter flow	ü Increase of Nusselt number: 31.28% ü Increase of friction factor: 23% ü Significant improvement in the performance parameters of the heat exchanger with a rise in volume concentration of the nanoparticle
Kumar, Bhramara [169]	Experimental Longitudinal strip insert *Re*: 15,000–30,000 Nanofluid: Fe_3O_4, mean diameter 36 nm, base fluid: water, concentration: 0.005, 0.01, 0.03 and 0.06% Inner: hot nanofluid, temperature: 60 °C Outer: cold water, temperature: 29 °C Counter flow	ü Increase of Nusselt number: 41.29% ü Increase of friction factor: 26.7% ü Heat transfer increases with increasing values of particle concentration, Reynolds number and with decreasing values of the aspect ratio of the longitudinal strip insert

combination of nanofluid and turbulator insertion is about 248%, 206%, and 181%, respectively. In the turbulator insertion technique, an external element in the tube gives a high friction factor. While in the geometry change technique, the increment of friction factor is because of the modification in tubes' wall. Nanofluids have the lowest friction factor by an average of 31% because there is no change or elements hindering the fluid flow. The increase in friction factor is because of an increase in fluid viscosity.

According to the thermal performance factor equation, the thermal performance factor is the ratio of heat transfer enhancement to friction factor increment. It can be concluded that using nanofluid and the combination of nanofluids and turbulator insertion have the best thermal performance factor with the extended surface area the lowest

thermal performance factor.

The standard deviation and box and whisker diagram were used to show the dispersion of heat transfer and friction factor augmentation data of each technique (Table 7 and Fig. 18). Among these five techniques, the combination of turbulator insertion and nanofluid technique has the highest heat transfer standard deviation by an average value of approximately 132. From the standard deviation, minimum, maximum and median values, it can be concluded that the potential for the increase of the average heat transfer for this technique is extensive. The extended surface area and turbulator insertion techniques are rated second and third respectively with approximate standard deviation heat transfer averages of 81 and 79. The average heat transfer standard deviation decreases respectively for the extended surface area, turbulator
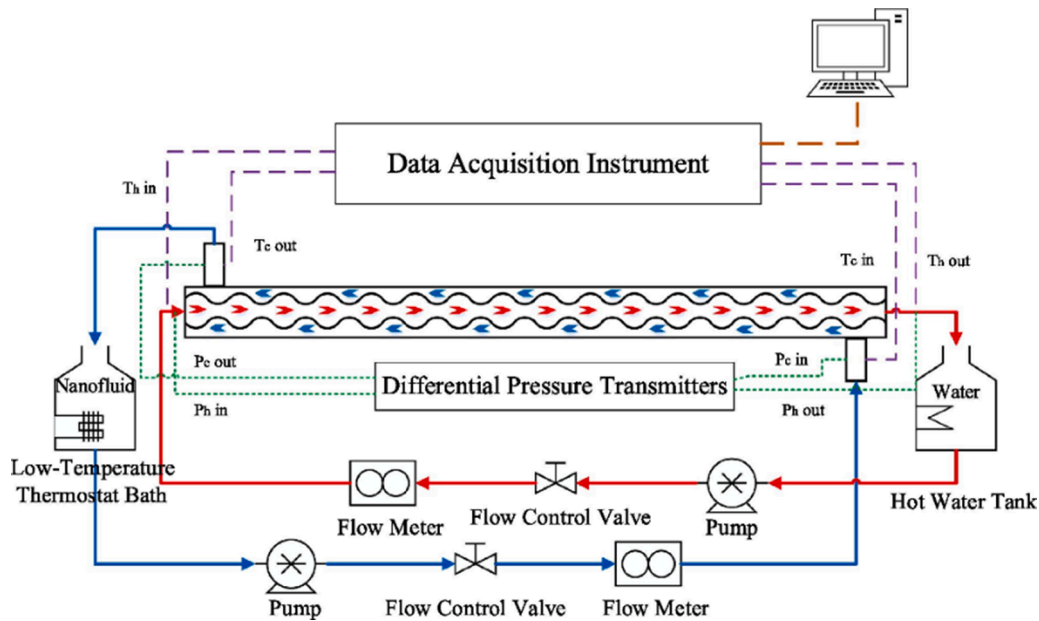
Fig. 16. Schematic diagram of the experimental system [179].

insertion, geometry change and nanofluids. It can be concluded that decreasing the standard deviation is accompanied by a decrease in the potential of increased heat transfer for that technique. The reduction in the range of data for the heat transfer augmentation can be seen in Fig. 18. by the minimum and maximum value of data. The standard deviation for friction factor has a high value for all techniques except nanofluid. This means that the range of friction factor increment for these techniques is extensive, especially in the extended surface area. The range of friction factors varies extensively by the occupation of the flow area in the tube in the extended surface area.

6. Conclusion

The present review article has focused on different passive methods of heat transfer and friction factor enhancement in DTHEs. There are different enhancement techniques in the passive method that can improve thermal performance in DTHEs: turbulators insertion, extended surface (fin), geometry change, and using nanofluids. All these techniques aim to improve heat transfer rate by reducing the thermal boundary layer and modifying thermal properties. The conclusions are:

- Generally, the heat transfer rate increases by increasing the Reynolds number in all techniques.
- Twisted tape inserts with a cut increases the heat transfer more than without the cut.
- The effect of a coil-wire insert on the enhancement of heat transfer decreases as the Reynolds number increases.
- By decreasing the pitch of the coil, twisted tape, and helical insertion, the heat transfer rate and pressure drop increases.
- The extended surface area (fin) technique has the worst effect on the pressure drop and friction factor.
- Using nanofluids in combination with other techniques is more effective than using it alone.
  Using nanofluids provide the best thermal performance factor in DTHEs.
- Using nanofluids with turbulator insertion has the greatest enhancement in the heat transfer rate.
- Turbulators insertion has a higher heat transfer enhancement in low Reynolds numbers than in higher Reynolds numbers. This is due to the intensification of turbulence. At the laminar regime, the disturbance is low, and the turbulator insertion can significantly affect

perturbation. However, in the turbulent regime, the flow already has turbulence, so the turbulator insertion has an insignificant effect on the perturbations.
- Both inner and outer tube modifications have a higher heat transfer rate and friction factor in comparison to a modified inner tube.
- Generally, in turbulator insertion and geometry change techniques, the greater the friction created, the higher the heat transfer rate.
- It is better to use nanofluids in applications that need low friction factors.
- The potential of the heat transfer enhancement is highest for the combination of turbulator insertion and nanofluid technique based on the standard deviation because this technique uses the beneficial effects of both techniques simultaneously.
- Based on standard deviation, the friction factor increment range is more extensive in comparison to the heat transfer increment range. It means the potential of the friction factor increment for each technique is higher than the heat transfer enhancement.
- Except for the nanofluid technique, almost all other techniques have a higher average standard deviation friction factor value than the corresponding average standard deviation heat transfer.

Many researchers have exhaustively explored the use of turbulators insertion, geometry change, and nanofluids to enhance the heat transfer characteristics in DTHEs. However, the areas below have not yet been explored in DTHEs and could be the focus of new research.

- Investigation of different techniques separately and comparing the results precisely to each other to see which technique has the better heat transfer rate and friction factor.
- Investigation of the turbulator insertion, extended surface, geometry change and nanofluids techniques in the transient regime.
- Investigation of the turbulator insertion, extended surface, geometry change and nanofluid techniques in different working fluids (other than water) and an extensive range of working fluid temperatures.
- Focusing on the impact of different techniques on friction factor and pressure drop.
- Investigation of different combination techniques, especially turbulator insertion and geometry change, turbulator insertion and extended surface, nanofluids and geometry change, geometry change and extended surface and nanofluids and extended surface area.

Table 6

Summary of information on the combination of different nanofluids and geometry change, and their effects compared to pure water and a conventional DTHE.

Author	Conditions	Findings
Qi, Luo [179]	Experimental Corrugated tube *Re*: 3000–12,000 Nanofluid: TiO_2, base fluid: water, concentration: 0.1, 0.3 and 0.5% Inner: hot water, temperature: 40 °C Outer: cold nanofluid, temperature: 20 °C Counter flow	ü Increase of heat transfer: 14.8% at concentration 0.5% ü Increase of the pressure drop: up to 51.9% ü The number of transfer unit (NTU) and effectiveness decrease firstly and then increase with the increase of Reynolds number ü When nanofluid is in the shell-side, the comprehensive performance index is stronger
Khanmohammadi, Rahimi [221]	Numerical Spiral tube *Re*: 10,000–50,000 Nanofluid: TiO_2, mean diameter 25 nm, base fluid: water, concentration: 0.1, 0.2, and 0.3% Inner: cold nanofluid, temperature: 30 °C Outer: hot water, temperature: 50 °C Counter flow	ü The increase of heat transfer: up to 6% ü The increase of friction factor: up to 2% ü The friction factor increases with increase of spiral diameter ü With increasing the concentration, the temperature increases and the temperature contour became uniform because of turbulence of the boundary layer due to adding nanoparticles
Kumar and Chandrasekar [222]	Experimental Helical coiled tube *Re*: laminar flow Nanofluid: multiwall carbon nanotube, mean diameter 50–80 nm, base fluid: water, concentration: 0.2, 0.4, and 0.6% Inner: cold nanofluid Outer: hot water Parallel flow	ü Increase of heat transfer: 35% ü Increase of friction factor: 40%
Huminic and Huminic [223]	Numerical Helical tube *Re* laminar flow Nanofluid: Cu and TiO_2, mean diameter 24 nm, base fluid: water, concentration: 0.5–3% Inner: hot nanofluid, temperature: 80 °C Outer: cold water, temperature: 10 °C Counter flow	ü Increase of heat transfer rate: 19% ü The convective heat transfer coefficients of the nanofluids and water increased with increasing of the mass flow rate and with the Dean number
Wu, Wang [224]	Experimental Helical coiled tube *Re*: 1000–15,000 Nanofluid: Al_2O_3, mean diameter 40 nm, base fluid: water, concentration: 0.20, 0.56, 1.02, 1.50, and 1.88% Inner: hot nanofluid, temperature: 28 °C Outer: cold water, temperature: 5.5 °C Counter flow	ü Increase of heat transfer: 3.43% ü The apparent friction factor decreases with *Re* when *Re*<6000 and increases with *Re* when *Re*>6000 ü Additional possible effects of nanoparticles, e.g., Brownian motion, thermophoresis and diffusiophoresis, on the convective heat transfer characteristics of the nanofluids are insignificant compared to the dominant thermophysical properties of the nanofluids
Aly [225]	Numerical Coiled tube *Re*: 5000–30,000 Nanofluid: Al_2O_3, mean diameter 40 nm, base fluid: water, concentration: 0.5, 1, 2% Inner: hot nanofluid, temperature: 50 °C Outer: cold water, temperature: 20 °C Counter flow	ü Increase of heat transfer coefficient: 30% ü Increase of pressure drop: 17% ü The heat transfer coefficient increases by increasing the coil diameter and nanoparticles volume concentration ü The friction factor increases with the increase in curvature ratio, and pressure drop penalty is negligible when increasing the nanoparticles volume concentration
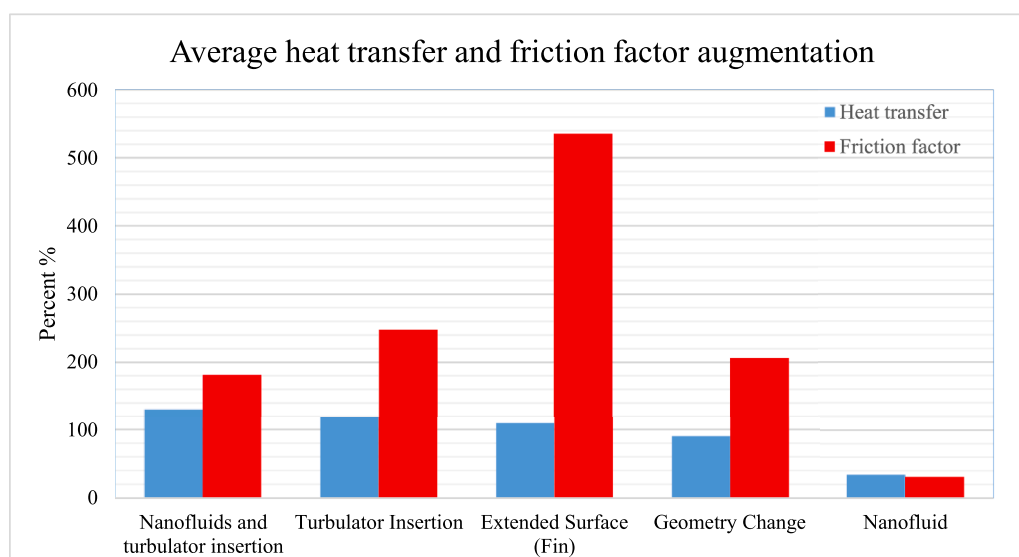
Fig. 17. Average heat transfer and friction factor augmentation of different techniques.

Table 7

Average enhancement of heat transfer and friction factor and standard deviation of different techniques.

Technique	Standard deviation	
	Heat transfer	Friction factor
Nanofluids and turbulator insertion	131.70	244.91
Extended surface (fin)	81.28	581.58
Turbulator insertion	78.80	157.66
Geometry change	54.28	194.71
Nanofluid	18.30	18.21
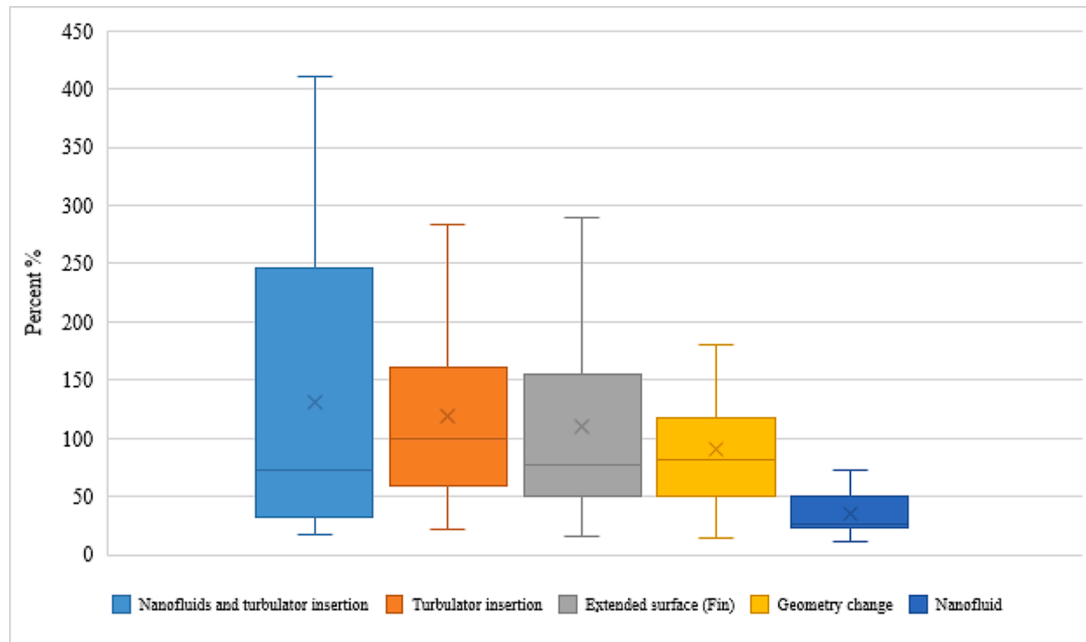
Fig.. 18. Heat transfer enhancement of different techniques (box and whisker plot).

- Investigation of a combination of three or four different techniques together.

Declaration of Competing Interest

The authors declare that they have no known competing financial interests or personal relationships that could have appeared to influence the work reported in this paper.

Data availability

No data was used for the research described in the article.

Supplementary materials

Supplementary material associated with this article can be found, in the online version, at doi:10.1016/j.ijft.2023.100282.

References

[1] S. Kakac, H. Liu, A. Pramuanjaroenkij, Heat exchangers: selection, rating, and Thermal Design, CRC press, 2002.

[2] R.K. Shah, D.P. Sekulic, Fundamentals of Heat Exchanger Design, John Wiley & Sons, 2003.

[3] H. Mohammed, H.A. Hasan, M. Wahid, Heat transfer enhancement of nanofluids in a double pipe heat exchanger with louvered strip inserts, Int. Commun. Heat Mass Transfer 40 (2013) 36–46.

[4] R. Andrzejczyk, T. Muszynski, P. Kozak, Experimental and computational fluid dynamics studies on straight and U-bend double tube heat exchangers with active and passive enhancement methods, Heat Transfer Eng. 42 (3–4) (2021) 167–180.

[5] F. Morris, W.G. Whitman, Heat transfer for oils and water in pipes1, Indus. Eng. Chem. 20 (3) (1928) 234–240.

[6] P. Naphon, Heat transfer and pressure drop in the horizontal double pipes with and without twisted tape insert, Int. Commun. Heat Mass Transfer 33 (2) (2006) 166–175.

[7] J. Córcoles, et al., Numerical and experimental study of the heat transfer process in a double pipe heat exchanger with inner corrugated tubes, Int. J. Therm. Sci. 158 (2020), 106526.

[8] C.V.M. Braga, F.E.M. Saboya, Turbulent heat transfer, pressure drop and fin efficiency in annular regions with continuous longitudinal rectangular fins, Exp. Therm Fluid Sci. 20 (2) (1999) 55–65.

[9] B.-.H. Chun, H.U. Kang, S.H. Kim, Effect of alumina nanoparticles in the fluid on heat transfer in double-pipe heat exchanger system, Korean J. Chem. Eng. 25 (5) (2008) 966–971.

[10] C. Yildiz, Y. Biçer, D. Pehlivan, Heat transfers and pressure drops in rotating helical pipes, Appl. Energy 50 (1) (1995) 85–94.

[11] M. Legay, et al., Improvement of heat transfer by means of ultrasound: application to a double-tube heat exchanger, Ultrason. Sonochem. 19 (6) (2012) 1194–1200.

[12] H.H. Habeeb, R.A. Khalefa, S. Kaska, Performance Enhancement of the Vertical Double Pipe Heat Exchanger by Applying of Bubbling Generation on the Shell Side, Kirkuk Univ. J./Sci. Stud. (KUJSS) 13 (1) (2018) 156–171.

[13] C. Maradiya, J. Vadher, R. Agarwal, The heat transfer enhancement techniques and their Thermal Performance Factor, Beni Suef Univ. J. Basic Appl. Sci. 7 (1) (2018) 1–21.

[14] M. Omidi, M. Farhadi, M. Jafari, A comprehensive review on double pipe heat exchangers, Appl. Therm. Eng. 110 (2017) 1075–1090.

[15] W. El-Maghlany, et al., Experimental study for double pipe heat exchanger with rotating inner pipe, Int. J. Adv. Sci. Tech. Res. 4 (2) (2012) 507–524.

[16] Z. Zhang, et al., Heat transfer enhancement in double-pipe heat exchanger by means of rotor-assembled strands, Chem. Eng. Process. 60 (2012) 26–33.

[17] S. Anitha, K. Loganathan, M. Pichumani, Approaches for modelling of industrial energy systems: correlation of heat transfer characteristics between

magnetohydrodynamics hybrid nanofluids and performance analysis of industrial length-scale heat exchanger, J. Therm. Anal. Calorim. (2020) 1–16.

[18] S. Liu, M. Sakr, A comprehensive review on passive heat transfer enhancements in pipe exchangers, Renew. Sustain. Energy Rev. 19 (2013) 64–81.

[19] M. Sheikholeslami, M. Gorji-Bandpy, D.D. Ganji, Review of heat transfer enhancement methods: focus on passive methods using swirl flow devices, Renew. Sustain. Energy Rev. 49 (2015) 444–469.

[20] P. Bharadwaj, A.D. Khondge, A.W. Date, Heat transfer and pressure drop in a spirally grooved tube with twisted tape insert, Int. J. Heat Mass Transf. 52 (7) (2009) 1938–1944.

[21] T. Alam, M.-H. Kim, A comprehensive review on single phase heat transfer enhancement techniques in heat exchanger applications, Renew. Sustain. Energy Rev. 81 (2018) 813–839.

[22] N. Targui, H. Kahalerras, Analysis of a double pipe heat exchanger performance by use of porous baffles and pulsating flow, Energy Convers. Manage. 76 (2013) 43–54.

[23] W. Duangthongsuk, S. Wongwises, An experimental investigation of the heat transfer and pressure drop characteristics of a circular tube fitted with rotating turbine-type swirl generators, Exp. Therm Fluid Sci. 45 (2013) 8–15.

[24] O. Shewale, et al., Experimental investigation of double pipe heat exchanger with helical fins on the inner rotating tube, Int. J. Res. Eng. Technol. 3 (7) (2014) 98–102.

[25] O. Keklikcioglu, V. Ozceyhan, A review of heat transfer enhancement methods using coiled wire and twisted tape inserts, Heat Transf. Models Methods Appl. (2018) 199–217.

[26] H.H. Hamed, et al., The effect of using compound techniques (passive and active) on the double pipe heat exchanger performance, Egypt. J. Chem. 64 (6) (2021) 2797–2802.

[27] V.D. Zimparov, V.M. Petkov, Compound heat transfer enhancement by a combination of spirally corrugated tubes with a twisted tape, in: International Heat Transfer Conference Digital Library, Begel House Inc, 2002.

[28] M. Bahiraei, N. Mazaheri, M. Hanooni, Performance enhancement of a triple-tube heat exchanger through heat transfer intensification using novel crimped-spiral ribs and nanofluid: a two-phase analysis, Chem. Eng. Process. Proc. Intensific. 160 (2021), 108289.

[29] C. Yildiz, Y. Bíçer, D. Pehlívan, Influence of fluid rotation on the heat transfer and pressure drop in double-pipe heat exchangers, Appl. Energy 54 (1) (1996) 49–56.

[30] E.F. Akyürek, et al., Experimental analysis for heat transfer of nanofluid with wire coil turbulators in a concentric tube heat exchanger, Results Phys. 9 (2018) 376–389.

[31] S.M. HM, R.N. Hegde, Investigations on the effect of disturbed flow using differently configured turbulators and Alumina nanofluid as a coolant in a double tube heat exchanger, Exp. Heat Transf. 35 (3) (2022) 282–307.

[32] R. Andrzejczyk, T. Muszynski, P. Kozak, Experimental investigation of heat transfer enhancement in straight and U-bend double-pipe heat exchanger with wire insert, Chem. Eng. Process. Proc. Intensific. 136 (2019) 177–190.

[33] A. Ponshanmugakumar, R. Rajavel, Enhancement of heat transfer in double pipe heat exchanger, Mater. Today: Proc. 16 (2019) 706–713.

[34] H. Karakaya, A. Durmuş, Heat transfer and exergy loss in conical spring turbulators, Int. J. Heat Mass Transf. 60 (2013) 756–762.

[35] P. Durga Prasad, A. Gupta, Augmentation of heat transfer and pressure drop characteristics inside a double pipe U-Tube heat exchanger by using twisted tape inserts. Emerging Trends in Science, Engineering and Technology, Springer, 2012, pp. 33–45.

[36] C. Yildiz, Y. Biçer, D. Pehlivan, Effect of twisted strips on heat transfer and pressure drop in heat exchangers, Energy Convers. Manage. 39 (3–4) (1998) 331–336.

[37] E.K. Akpinar, et al., Heat transfer enhancements in a concentric double pipe exchanger equipped with swirl elements, Int. Commun. Heat Mass Transfer 31 (6) (2004) 857–868.

[38] C. Gnanavel, R. Saravanan, M. Chandrasekaran, Heat transfer enhancement through nano-fluids and twisted tape insert with rectangular cut on its rib in a double pipe heat exchanger, Mater. Today: Proc. 21 (2020) 865–869.

[39] N. Mashoofi, et al., Fabrication method and thermal-frictional behavior of a tube-in-tube helically coiled heat exchanger which contains turbulator, Appl. Therm. Eng. 111 (2017) 1008–1015.

[40] M.M.K. Bhuiya, et al., Performance assessment in a heat exchanger tube fitted with double counter twisted tape inserts, Int. Commun. Heat Mass Transfer 50 (2014) 25–33.

[41] S. Eiamsa-ard, C. Thianpong, P. Promvonge, Experimental investigation of heat transfer and flow friction in a circular tube fitted with regularly spaced twisted tape elements, Int. Commun. Heat Mass Transfer 33 (10) (2006) 1225–1233.

[42] P. Promvonge, Thermal performance in circular tube fitted with coiled square wires, Energy Convers. Manage. 49 (5) (2008) 980–987.

[43] S.W. Chang, Y.J. Jan, J.S. Liou, Turbulent heat transfer and pressure drop in tube fitted with serrated twisted tape, Int. J. Therm. Sci. 46 (5) (2007) 506–518.

[44] M. Nakhchi, I. Esfahani, K. Kim, Numerical study of turbulent flow inside heat exchangers using perforated louvered strip inserts, Int. J. Heat Mass Transf. 148 (2020), 119143.

[45] E.Z. Ibrahim, Augmentation of laminar flow and heat transfer in flat tubes by means of helical screw-tape inserts, Energy Convers. Manage. 52 (1) (2011) 250–257.

[46] P. Naphon, Effect of coil-wire insert on heat transfer enhancement and pressure drop of the horizontal concentric tubes, Int. Commun. Heat Mass Transfer 33 (6) (2006) 753–763.

[47] S. Eiamsa-ard, et al., Turbulent flow heat transfer and pressure loss in a double pipe heat exchanger with louvered strip inserts, Int. Commun. Heat Mass Transfer 35 (2) (2008) 120–129.

[48] S. Zhang, et al., Performance evaluation of a double-pipe heat exchanger fitted with self-rotating twisted tapes, Appl. Therm. Eng. 158 (2019), 113770.

[49] E.K. Akpinar, Y. Bicer, Investigation of heat transfer and exergy loss in a concentric double pipe exchanger equipped with swirl generators, Int. J. Therm. Sci. 44 (6) (2005) 598–607.

[50] R. Aridi, et al., CFD analysis on the spatial effect of vortex generators in concentric tube heat exchangers–A comparative study, Int. J. Thermofluids 16 (2022), 100247.

[51] E.K. Akpinar, Evaluation of heat transfer and exergy loss in a concentric double pipe exchanger equipped with helical wires, Energy Convers. Manage. 47 (18) (2006) 3473–3486.

[52] A.S. Yadav, Effect of half length twisted-tape turbulators on heat transfer and pressure drop characteristics inside a double pipe u-bend heat exchanger, JJMIE 3 (1) (2009) 17–22.

[53] S. Eiamsa-ard, et al., Heat transfer enhancement in a tube using delta-winglet twisted tape inserts, Appl. Therm. Eng. 30 (4) (2010) 310–318.

[54] S.C. Shashank, S. Taji, Experimental studies on effect of coil wire insert on heat transfer enhancement and friction factor of double pipe heat exchanger, Int. J. Comput. Eng. Res. 3 (5) (2013).

[55] M. Sheikholeslami, et al., Thermal management of double-pipe air to water heat exchanger, Energy Build. 88 (2015) 361–366.

[56] J. Moya-Rico, et al., Experimental characterization of a double tube heat exchanger with inserted twisted tape elements, Appl. Therm. Eng. 174 (2020), 115234.

[57] Q.J. Slaiman, A.N. Znad, Enhancement of Heat Transfer in The Tube-Sid of A Double Pipe Heat Exchanger by Wire Coils, Al-Nahrain J. Eng. Sci. 16 (1) (2013) 51–57.

[58] A. García, P.G. Vicente, A. Viedma, Experimental study of heat transfer enhancement with wire coil inserts in laminar-transition-turbulent regimes at different Prandtl numbers, Int. J. Heat Mass Transf. 48 (21) (2005) 4640–4651.

[59] S. Padmanabhan, et al., Heat transfer analysis of double tube heat exchanger with helical inserts, Mater. Today: Proc. (2021).

[60] S. Pourahmad, S.M. Pesteei, Effectiveness-NTU analyses in a double tube heat exchanger equipped with wavy strip considering various angles, Energy Convers. Manage. 123 (2016) 462–469.

[61] P. Murugesan, et al., Heat transfer and pressure drop characteristics in a circular tube fitted with and without V-cut twisted tape insert, Int. Commun. Heat Mass Transfer 38 (3) (2011) 329–334.

[62] A.T. Wijayanta, B. Kristiawan, M. Aziz, Internal flow in an enhanced tube having square-cut twisted tape insert, Energies 12 (2) (2019) 306.

[63] Z. Iqbal, K. Syed, M. Ishaq, Fin design for conjugate heat transfer optimization in double pipe, Int. J. Therm. Sci. 94 (2015) 242–258.

[64] Z. Iqbal, K. Syed, M. Ishaq, Optimal fin shape in finned double pipe with fully developed laminar flow, Appl. Therm. Eng. 51 (1–2) (2013) 1202–1223.

[65] K.S. Syed, M. Ishaq, M. Bakhsh, Laminar convection in the annulus of a double-pipe with triangular fins, Comput. Fluids 44 (1) (2011) 43–55.

[66] H. Kahalerras, N. Targui, Numerical analysis of heat transfer enhancement in a double pipe heat exchanger with porous fins, Int. J. Numer. Methods Heat Fluid Flow (2008).

[67] R.L. Mohanty, S. Bashyam, D. Das, Numerical analysis of double pipe heat exchanger using heat transfer augmentation techniques, Int. J. Plast. Technol. 18 (3) (2014) 337–348.

[68] L. Zhang, et al., Effects of the arrangement of triangle-winglet-pair vortex generators on heat transfer performance of the shell side of a double-pipe heat exchanger enhanced by helical fins, Heat Mass Transf. 53 (1) (2017) 127–139.

[69] M.A. Hussein, V.M. Hameed, Experimental investigation on the effect of semi-circular perforated baffles with semi-circular fins on air–water double pipe heat exchanger, Arab. J. Sci. Eng. 47 (5) (2022) 6115–6124.

[70] N.S. Reddy, K. Rajagopal, P. Veena, Experimental investigation of heat transfer enhancement of a double pipe heat exchanger with helical fins in the annulus side, Int. J. Dyn. Fluids 13 (2) (2017) 285–293.

[71] V. Mathanraj, et al., Experimental investigation on heat transfer in double pipe heat exchanger employing triangular fins, in: IOP Conference Series: Materials Science and Engineering, IOP Publishing, 2018.

[72] V.M. Hameed, B.M. Essa, Turbulent flow heat transfer and pressure loss in a double pipe heat exchanger with triangular fins, Int. J. Energy Environ. 7 (2) (2016) 149.

[73] A.B. Colaço, et al., Maximizing the thermal performance index applying evolutionary multi-objective optimization approaches for double pipe heat exchanger, Appl. Therm. Eng. 211 (2022), 118504.

[74] Z. Iqbal, K. Syed, M. Ishaq, Optimal convective heat transfer in double pipe with parabolic fins, Int. J. Heat Mass Transf. 54 (25–26) (2011) 5415–5426.

[75] R. Raj, N.S. Lakshman, Y. Mukkamala, Single phase flow heat transfer and pressure drop measurements in doubly enhanced tubes, Int. J. Therm. Sci. 88 (2015) 215–227.

[76] B. Jalili, et al., Novel usage of the curved rectangular fin on the heat transfer of a double-pipe heat exchanger with a nanofluid, Case Stud. Therm. Eng. (2022), 102086.

[77] M. Iqbal, K. Syed, Thermally developing flow in finned double-pipe heat exchanger, Int. J. Num. Methods Fluids 65 (10) (2011) 1145–1159.

[78] L. Wang, Y. Lei, S. Jing, Performance of a Double-Tube Heat Exchanger with Staggered Helical Fins, Chem. Eng. Technol. 45 (5) (2022) 953–961.

[79] K. Syed, Z. Iqbal, M. Ishaq, Optimal configuration of finned annulus in a double pipe with fully developed laminar flow, Appl. Therm. Eng. 31 (8–9) (2011) 1435–1446.

[80] W. Ahmad, et al., Numerical study of conjugate heat transfer in a double-pipe with exponential fins using DGFEM, Appl. Therm. Eng. 111 (2017) 1184–1201.

[81] J. Taborek, Double-pipe and multitube heat exchangers with plain and longitudinal finned tubes, Heat Transfer Eng. 18 (2) (1997) 34–45.

[82] E. Cao, Heat Transfer in Process Engineering, McGraw-Hill Education, 2010.

[83] L. Zhang, et al., Compound Heat Transfer Enhancement For Shell Side of Double-Pipe Heat Exchanger By Helical Fins and Vortex Generators, 48, Heat and Mass Transfer, 2012, pp. 1113–1124.

[84] L. Zhang, et al., Fluid flow characteristics for shell side of double-pipe heat exchanger with helical fins and pin fins, Exp. Therm Fluid Sci. 36 (2012) 30–43.

[85] M. Kind, et al., VDI Heat Atlas, Springer, 2010.

[86] R. Eason, Y. Bayazitoglu, A. Meade, Enhancement of heat transfer in square helical ducts, Int. J. Heat Mass Transf. 37 (14) (1994) 2077–2087.

[87] L. Zhang, et al., Heat transfer enhancement by streamlined winglet pair vortex generators for helical channel with rectangular cross section, Chem. Eng. Process. Proc. Intensific. 147 (2020), 107788.

[88] A. El Maakoul, et al., Numerical investigation of thermohydraulic performance of air to water double-pipe heat exchanger with helical fins, Appl. Therm. Eng. 127 (2017) 127–139.

[89] A. El Maakoul, et al., Performance enhancement of finned annulus using surface interruptions in double-pipe heat exchangers, Energy Convers. Manage. 210 (2020), 112710.

[90] D. Majidi, H. Alighardashi, F. Farhadi, Experimental studies of heat transfer of air in a double-pipe helical heat exchanger, Appl. Therm. Eng. 133 (2018) 276–282.

[91] K.S. Syed, et al., Numerical study of an innovative design of a finned double-pipe heat exchanger with variable fin-tip thickness, Energy Convers. Manage. 98 (2015) 69–80.

[92] A. Zohir, M. Habib, M. Nemitallah, Heat transfer characteristics in a double-pipe heat exchanger equipped with coiled circular wires, Exp. Heat Transfer 28 (6) (2015) 531–545.

[93] M. Sheikholeslami, M. Gorji-Bandpy, D.D. Ganji, Experimental study on turbulent flow and heat transfer in an air to water heat exchanger using perforated circular-ring, Exp. Therm Fluid Sci. 70 (2016) 185–195.

[94] M. Sheikholeslami, M. Gorji-Bandpy, D.D. Ganji, Effect of discontinuous helical turbulators on heat transfer characteristics of double pipe water to air heat exchanger, Energy Convers. Manage. 118 (2016) 75–87.

[95] V.K. Karanth, K. Murthy, Numerical study of heat transfer in a finned double pipe heat exchanger, World J. Modell. Simul. 11 (1) (2015) 43–54.

[96] A. El Maakoul, et al., Numerical design and investigation of heat transfer enhancement and performance for an annulus with continuous helical baffles in a double-pipe heat exchanger, Energy Convers. Manage. 133 (2017) 76–86.

[97] N. Sreedhard, G. Varghese, Analysis of longitudinal fin patterns in a concentric double tube heat exchanger using LMTD and CFD techniques, Int. J. Appl. Eng. Res. 12 (17) (2017) 6471–6479.

[98] Z. Zhang, Z. Yu, X. Fang, An experimental heat transfer study for helically flowing outside petal-shaped finned tubes with different geometrical parameters, Appl. Therm. Eng. 27 (1) (2007) 268–272.

[99] M.R. Salem, et al., Experimental investigation on the hydrothermal performance of a double-pipe heat exchanger using helical tape insert, Int. J. Therm. Sci. 124 (2018) 496–507.

[100] S. Yadav, S.K. Sahu, Heat transfer augmentation in double pipe water to air counter flow heat exchanger with helical surface disc turbulators, Chem. Eng. Process. Proc. Intensific. 135 (2019) 120–132.

[101] M. Sheikholeslami, D. Ganji, Heat transfer improvement in a double pipe heat exchanger by means of perforated turbulators, Energy Convers. Manage. 127 (2016) 112–123.

[102] K. Shaji, Numerical analysis on a double pipe heat exchanger with twisted tape induced swirl flow on both sides, Procedia Technol. 24 (2016) 436–443.

[103] M. Yassin, et al., Heat transfer augmentation for annular flow due to rotation of inner finned pipe, Int. J. Therm. Sci. 134 (2018) 653–660.

[104] M. Ravikumar, Y.A. Raj, Investigation of fin profile on the performance of the shell and tube heat exchanger, Mater. Today: Proc. 45 (2021) 7910–7916.

[105] S. Sivalakshmi, M. Raja, G. Gowtham, Effect of helical fins on the performance of a double pipe heat exchanger, Mater. Today: Proc. 43 (2021) 1128–1131.

[106] A.A.R. Darzi, M. Farhadi, K. Sedighi, Experimental investigation of convective heat transfer and friction factor of Al2O3/water nanofluid in helically corrugated tube, Exp. Therm Fluid Sci. 57 (2014) 188–199.

[107] S. Vaezi, S. Karbalaee, P. Hanafizadeh, Effect of aspect ratio on heat transfer enhancement in alternating oval double pipe heat exchangers, Appl. Therm. Eng. 125 (2017) 1164–1172.

[108] S. Yang, L. Zhang, H. Xu, Experimental study on convective heat transfer and flow resistance characteristics of water flow in twisted elliptical tubes, Appl. Therm. Eng. 31 (14–15) (2011) 2981–2991.

[109] X.-h. Tan, et al., Heat transfer and pressure drop performance of twisted oval tube heat exchanger, Appl. Therm. Eng. 50 (1) (2013) 374–383.

[110] J.-A. Meng, et al., Experimental study on convective heat transfer in alternating elliptical axis tubes, Exp. Therm Fluid Sci. 29 (4) (2005) 457–465.

[111] V. Kumar, et al., Pressure drop and heat transfer study in tube-in-tube helical heat exchanger, Chem. Eng. Sci. 61 (13) (2006) 4403–4416.

[112] X. Tang, X. Dai, D. Zhu, Experimental and numerical investigation of convective heat transfer and fluid flow in twisted spiral tube, Int. J. Heat Mass Transf. 90 (2015) 523–541.

[113] J.M. Gorman, K.R. Krautbauer, E.M. Sparrow, Thermal and fluid flow first-principles numerical design of an enhanced double pipe heat exchanger, Appl. Therm. Eng. 107 (2016) 194–206.

[114] A. Asadi, et al., Numerical analysis of turbulence-inducing elements with various geometries and utilization of hybrid nanoparticles in a double pipe heat exchanger, Alexandria Eng. J. 61 (5) (2022) 3633–3644.

[115] T.J. Rennie, V.G. Raghavan, Numerical studies of a double-pipe helical heat exchanger, Appl. Therm. Eng. 26 (11–12) (2006) 1266–1273.

[116] D. Huu-Quan, et al., 3D numerical investigation of turbulent forced convection in a double-pipe heat exchanger with flat inner pipe, Appl. Therm. Eng. 182 (2021), 116106.

[117] D. Brough, et al., Development and validation of a TRNSYS type to simulate heat pipe heat exchangers in transient applications of waste heat recovery, Int. J. Thermofluids 9 (2021), 100056.

[118] S. Pesteei, et al., Numerical investigation on the effect of a modified corrugated double tube heat exchanger on heat transfer enhancement and exergy losses, Int. J. Heat Technol. 35 (2) (2017) 243–248.

[119] H.S. Dizaji, S. Jafarmadar, F. Mobadersani, Experimental studies on heat transfer and pressure drop characteristics for new arrangements of corrugated tubes in a double pipe heat exchanger, Int. J. Therm. Sci. 96 (2015) 211–220.

[120] H.-Z. Han, et al., Multi-objective shape optimization of double pipe heat exchanger with inner corrugated tube using RSM method, Int. J. Therm. Sci. 90 (2015) 173–186.

[121] R. Yang, F.P. Chiang, An experimental heat transfer study for periodically varying-curvature curved-pipe, Int. J. Heat Mass Transf. 45 (15) (2002) 3199–3204.

[122] W.-.L. Chen, W.-.C. Dung, Numerical study on heat transfer characteristics of double tube heat exchangers with alternating horizontal or vertical oval cross section pipes as inner tubes, Energy Convers. Manage. 49 (6) (2008) 1574–1583.

[123] C. Luo, et al., Heat transfer enhancement in a novel annular tube with outer straight and inner twisted oval tubes, Symmetry (Basel) 12 (8) (2020) 1213.

[124] J.-A. Zambaux, et al., The effect of successive alternating wall deformation on the performance of an annular heat exchanger, Appl. Therm. Eng. 90 (2015) 286–295.

[125] M. Hashemian, et al., Enhancement of heat transfer rate with structural modification of double pipe heat exchanger by changing cylindrical form of tubes into conical form, Appl. Therm. Eng. 118 (2017) 408–417.

[126] M.A. Moawed, E. Ibrahim, A. Gomaa, Thermal performance of a pipe in pipe heat exchanger with sinusoidal inner pipe, Energy Convers. Manage. 49 (4) (2008) 678–686.

[127] R. Webb, Principles of Enhanced Heat Transfer, John Wiely & Sons. Inc., New York, 1994, pp. 293–294.

[128] R. Bhadouriya, A. Agrawal, S.V. Prabhu, Experimental and numerical study of fluid flow and heat transfer in an annulus of inner twisted square duct and outer circular pipe, Int. J. Therm. Sci. 94 (2015) 96–109.

[129] C. Luo, K. Song, Thermal performance enhancement of a double-tube heat exchanger with novel twisted annulus formed by counter-twisted oval tubes, Int. J. Therm. Sci. 164 (2021), 106892.

[130] H.S. Dizaji, S. Jafarmadar, S. Asaadi, Experimental exergy analysis for shell and tube heat exchanger made of corrugated shell and corrugated tube, Exp. Therm Fluid Sci. 81 (2017) 475–481.

[131] W. Wang, et al., Optimal design of a double pipe heat exchanger based on the outward helically corrugated tube, Int. J. Heat Mass Transf. 135 (2019) 706–716.

[132] S. Pethkool, et al., Turbulent heat transfer enhancement in a heat exchanger using helically corrugated tube, Int. Commun. Heat Mass Transfer 38 (3) (2011) 340–347.

[133] S. Laohalertdecha, S. Wongwises, The effects of corrugation pitch on the condensation heat transfer coefficient and pressure drop of R-134a inside horizontal corrugated tube, Int. J. Heat Mass Transf. 53 (13) (2010) 2924–2931.

[134] R. Webb, R. Narayanamurthy, P. Thors, Heat transfer and friction characteristics of internal helical-rib roughness, J. Heat Transf. 122 (1) (2000) 134–142.

[135] Z. Li, et al., Effect of internal helical-rib roughness on mixed convection flow and heat transfer in heated horizontal pipe flow of supercritical water, Int. J. Heat Mass Transf. 130 (2019) 1272–1287.

[136] H. Han, B. Li, W. Shao, Multi-objective optimization of outward convex corrugated tubes using response surface methodology, Appl. Therm. Eng. 70 (1) (2014) 250–262.

[137] S. Wongwises, M. Polsongkram, Condensation heat transfer and pressure drop of HFC-134a in a helically coiled concentric tube-in-tube heat exchanger, Int. J. Heat Mass Transf. 49 (23) (2006) 4386–4398.

[138] V. Kumar, et al., Numerical studies of a tube-in-tube helically coiled heat exchanger, Chem. Eng. Process. 47 (12) (2008) 2287–2295.

[139] L. Shao, et al., Condensation heat transfer of R-134A in horizontal straight and helically coiled tube-in-tube heat exchangers, J. Hydrodyn. Ser. B (English Ed.) 19 (6) (2007) 677–682.

[140] S.U. Choi, J.A. Eastman, Enhancing Thermal Conductivity of Fluids With Nanoparticles, Argonne National Lab., ILUnited States, 1995.

[141] Lee, S., et al., *Measuring thermal conductivity of fluids containing oxide nanoparticles.* 1999.

[142] W. Yu, et al., Review and comparison of nanofluid thermal conductivity and heat transfer enhancements, Heat Transfer Eng. 29 (5) (2008) 432–460.

[143] R. Saidur, K.Y. Leong, H.A. Mohammed, A review on applications and challenges of nanofluids, Renew. Sustain. Energy Rev. 15 (3) (2011) 1646–1668.

[144] N. Ali, J.A. Teixeira, A. Addali, A Review on Nanofluids: fabrication, Stability, and Thermophysical Properties, J. Nanomater. 2018 (2018), 6978130.

[145] L. Yang, et al., An updated review on the properties, fabrication and application of hybrid-nanofluids along with their environmental effects, J. Clean. Prod. 257 (2020), 120408.

[146] K.-F.V. Wong, T. Kurma, Transport properties of alumina nanofluids, Nanotechnology 19 (34) (2008), 345702.

[147] N. Kumar, S.S. Sonawane, Experimental study of Fe2O3/water and Fe2O3/ethylene glycol nanofluid heat transfer enhancement in a shell and tube heat exchanger, Int. Commun. Heat Mass Transfer 78 (2016) 277–284.

[148] J.G. Monroe, et al., On the energy harvesting and heat transfer ability of a ferro-nanofluid oscillating heat pipe, Int. J. Heat Mass Transf. 132 (2019) 162–171.

[149] V. Nageswara Rao, B.Ravi Sankar, Heat transfer and friction factor investigations of CuO nanofluid flow in a double pipe U-bend heat exchanger, Mater. Today: Proc. 18 (2019) 207–218.

[150] M.E. Nakhchi, J.A. Esfahani, CFD approach for two-phase CuO nanofluid flow through heat exchangers enhanced by double perforated louvered strip insert, Powder Technol. 367 (2020) 877–888.

[151] S.S.J. Aravind, S. Ramaprabhu, Graphene–multiwalled carbon nanotube-based nanofluids for improved heat dissipation, RSC Adv. 3 (13) (2013) 4199–4206.

[152] A.D. Manasrah, et al., Surface modification of carbon nanotubes with copper oxide nanoparticles for heat transfer enhancement of nanofluids, RSC Adv. 8 (4) (2018) 1791–1802.

[153] A.O. Borode, N.A. Ahmed, P.A. Olubambi, A review of heat transfer application of carbon-based nanofluid in heat exchangers, Nano-Struct. Nano-Objects 20 (2019), 100394.

[154] D.R. Karana, R.R. Sahoo, Performance effect on the TEG system for waste heat recovery in automobiles using ZnO and SiO2 nanofluid coolants, Heat Transf. Asian Res. 48 (1) (2019) 216–232.

[155] A.F. Niwalkar, J.M. Kshirsagar, K. Kulkarni, Experimental investigation of heat transfer enhancement in shell and helically coiled tube heat exchanger using SiO2/water nanofluids, Mater. Today: Proc. 18 (2019) 947–962.

[156] D. Huang, Z. Wu, B. Sunden, Effects of hybrid nanofluid mixture in plate heat exchangers, Exp. Therm. Fluid Sci. 72 (2016) 190–196.

[157] S. Anitha, et al., What dominates heat transfer performance of hybrid nanofluid in single pass shell and tube heat exchanger? Adv. Powder Technol. 30 (12) (2019) 3107–3117.

[158] S.K. Singh, J. Sarkar, Improving hydrothermal performance of hybrid nanofluid in double tube heat exchanger using tapered wire coil turbulator, Adv. Powder Technol. 31 (5) (2020) 2092–2100.

[159] S.A. Angayarkanni, J. Philip, Review on thermal properties of nanofluids: recent developments, Adv. Colloid Interface Sci. 225 (2015) 146–176.

[160] R.B. Ganvir, P.V. Walke, V.M. Kriplani, Heat transfer characteristics in nanofluid—a review, Renew. Sustain. Energy Rev. 75 (2017) 451–460.

[161] P.C. Mukesh Kumar, M. Chandrasekar, A review on helically coiled tube heat exchanger using nanofluids, Mater. Today: Proc. 21 (2020) 137–141.

[162] M. Awais, et al., Heat transfer and pressure drop performance of Nanofluid: a state-of- the-art review, Int. J. Thermofluids 9 (2021), 100065.

[163] Y. Xuan, Q. Li, Heat transfer enhancement of nanofluids, Int. J. Heat Fluid Flow 21 (1) (2000) 58–64.

[164] R.R. Riehl, S. Mancin, Estimation of thermophysical properties for accurate numerical simulation of nanofluid heat transfer applied to a loop heat pipe, Int. J. Thermofluids (2022), 100158.

[165] L.S. Sundar, et al., Experimental heat transfer, friction factor and effectiveness analysis of Fe3O4 nanofluid flow in a horizontal plain tube with return bend and wire coil inserts, Int. J. Heat Mass Transf. 109 (2017) 440–453.

[166] W. Duangthongsuk, S. Wongwises, Heat transfer enhancement and pressure drop characteristics of TiO2–water nanofluid in a double-tube counter flow heat exchanger, Int. J. Heat Mass Transf. 52 (7–8) (2009) 2059–2067.

[167] A.M. Hussein, Thermal performance and thermal properties of hybrid nanofluid laminar flow in a double pipe heat exchanger, Exp. Therm. Fluid Sci. 88 (2017) 37–45.

[168] N.R. Kumar, et al., Heat transfer, friction factor and effectiveness analysis of Fe3O4/water nanofluid flow in a double pipe heat exchanger with return bend, Int. Commun. Heat Mass Transfer 81 (2017) 155–163.

[169] N.R. Kumar, et al., Heat transfer, friction factor and effectiveness of Fe3O4 nanofluid flow in an inner tube of double pipe U-bend heat exchanger with and without longitudinal strip inserts, Exp. Therm. Fluid Sci. 85 (2017) 331–343.

[170] M.H. Esfe, et al., Heat transfer characteristics and pressure drop of COOH-functionalized DWCNTs/water nanofluid in turbulent flow at low concentrations, Int. J. Heat Mass Transf. 73 (2014) 186–194.

[171] A.A. Arani, J. Amani, Experimental study on the effect of TiO2–water nanofluid on heat transfer and pressure drop, Exp. Therm. Fluid Sci. 42 (2012) 107–115.

[172] M.H. Esfe, S. Saedodin, M. Mahmoodi, Experimental studies on the convective heat transfer performance and thermophysical properties of MgO–water nanofluid under turbulent flow, Exp. Therm. Fluid Sci. 52 (2014) 68–78.

[173] A.J.N. Khalifa, M.A. Banwan, Effect of volume fraction of γ-Al2O3 nanofluid on heat transfer enhancement in a concentric tube heat exchanger, Heat Transf. Eng. 36 (16) (2015) 1387–1396.

[174] R.S. Khedkar, S.S. Sonawane, K.L. Wasewar, Heat transfer study on concentric tube heat exchanger using TiO2–water based nanofluid, Int. Commun. Heat Mass Transfer 57 (2014) 163–169.

[175] M. Goodarzi, et al., Investigation of heat transfer performance and friction factor of a counter-flow double-pipe heat exchanger using nitrogen-doped, graphene-based nanofluids, Int. Commun. Heat Mass Transfer 76 (2016) 16–23.

[176] H.M. Maghrabie, et al., Intensification of heat exchanger performance utilizing nanofluids, Int. J. Thermofluids 10 (2021), 100071.

[177] W.M. El-Maghlany, et al., Experimental study of Cu–water nanofluid heat transfer and pressure drop in a horizontal double-tube heat exchanger, Exp. Therm. Fluid Sci. 78 (2016) 100–111.

[178] D. Han, W. He, F. Asif, Experimental study of heat transfer enhancement using nanofluid in double tube heat exchanger, Energy Procedia 142 (2017) 2547–2553.

[179] C. Qi, et al., Experimental study on the flow and heat transfer characteristics of nanofluids in double-tube heat exchangers based on thermal efficiency assessment, Energy Convers. Manage. 197 (2019), 111877.

[180] A. Zamzamian, et al., Experimental investigation of forced convective heat transfer coefficient in nanofluids of Al2O3/EG and CuO/EG in a double pipe and plate heat exchangers under turbulent flow, Exp. Therm Fluid Sci. 35 (3) (2011) 495–502.

[181] A.R. Darzi, M. Farhadi, K. Sedighi, Heat transfer and flow characteristics of Al2O3–water nanofluid in a double tube heat exchanger, Int. Commun. Heat Mass Transfer 47 (2013) 105–112.

[182] R. Aghayari, et al., Effect of nanoparticles on heat transfer in mini double-pipe heat exchangers in turbulent flow, Heat Mass Transfer 51 (3) (2015) 301–306.

[183] M. Sarafraz, F. Hormozi, Intensification of forced convection heat transfer using biological nanofluid in a double-pipe heat exchanger, Exp. Therm Fluid Sci. 66 (2015) 279–289.

[184] M.A.E.-M. Mohamed, A.J. Gutiérrez-Trashorras, E.B. Marigorta, Numerical investigation of heat transfer with nanofluids in concentric tube heat exchanger under transitional flow, Energy 1 (1) (2020).

[185] D. Zheng, et al., Heat transfer performance and friction factor of various nanofluids in a double-tube counter flow heat exchanger, Therm. Sci. (00) (2020) 280. -280.

[186] W. Duangthongsuk, S. Wongwises, An experimental study on the heat transfer performance and pressure drop of TiO2-water nanofluids flowing under a turbulent flow regime, Int. J. Heat Mass Transf. 53 (1–3) (2010) 334–344.

[187] D. Madhesh, S. Kalaiselvam, Experimental study on the heat transfer and flow properties of Ag–ethylene glycol nanofluid as a coolant, Heat Mass Transf. 50 (11) (2014) 1597–1607.

[188] D. Nagaraju, A.R. Mohammad, Effect of graphene-based nanofluid on heat transfer performance of alternate elliptical axis oval tube heat exchanger, Appl. Nanosci. 12 (6) (2022) 1839–1858.

[189] S.H. Hashemi Karouei, et al., Laminar heat transfer and fluid flow of two various hybrid nanofluids in a helical double-pipe heat exchanger equipped with an innovative curved conical turbulator, J. Therm. Anal. Calorim. 143 (2) (2021) 1455–1466.

[190] V. Mokkapati, C.-.S. Lin, Numerical study of an exhaust heat recovery system using corrugated tube heat exchanger with twisted tape inserts, Int. Commun. Heat Mass Transfer 57 (2014) 53–64.

[191] H. Maddah, et al., Experimental study of Al2O3/water nanofluid turbulent heat transfer enhancement in the horizontal double pipes fitted with modified twisted tapes, Int. J. Heat Mass Transf. 78 (2014) 1042–1054.

[192] M. Nakhchi, J. Esfahani, Numerical investigation of turbulent Cu-water nanofluid in heat exchanger tube equipped with perforated conical rings, Adv. Powder Technol. 30 (7) (2019) 1338–1347.

[193] O. Sadeghi, et al., Heat transfer and nanofluid flow characteristics through a circular tube fitted with helical tape inserts, Int. Commun. Heat Mass Transfer 71 (2016) 234–244.

[194] S. Suresh, K. Venkitaraj, P. Selvakumar, Comparative study on thermal performance of helical screw tape inserts in laminar flow using Al2O3/water and CuO/water nanofluids, Superlattices Microstruct. 49 (6) (2011) 608–622.

[195] K. Sharma, L.S. Sundar, P. Sarma, Estimation of heat transfer coefficient and friction factor in the transition flow with low volume concentration of Al2O3 nanofluid flowing in a circular tube and with twisted tape insert, Int. Commun. Heat Mass Transfer 36 (5) (2009) 503–507.

[196] K. Wongcharee, S. Eiamsa-Ard, Enhancement of heat transfer using CuO/water nanofluid and twisted tape with alternate axis, Int. Commun. Heat Mass Transfer 38 (6) (2011) 742–748.

[197] M. Naik, G.R. Janardana, L.S. Sundar, Experimental investigation of heat transfer and friction factor with water–propylene glycol based CuO nanofluid in a tube with twisted tape inserts, Int. Commun. Heat Mass Transfer 46 (2013) 13–21.

[198] W. Azmi, et al., Numerical validation of experimental heat transfer coefficient with SiO2 nanofluid flowing in a tube with twisted tape inserts, Appl. Therm. Eng. 73 (1) (2014) 296–306.

[199] S. Eiamsa-ard, K. Kiatkittipong, Heat transfer enhancement by multiple twisted tape inserts and TiO2/water nanofluid, Appl. Therm. Eng. 70 (1) (2014) 896–924.

[200] M. Naik, et al., Comparative study on thermal performance of twisted tape and wire coil inserts in turbulent flow using CuO/water nanofluid, Exp. Therm. Fluid Sci. 57 (2014) 65–76.

[201] W. Azmi, et al., Comparison of convective heat transfer coefficient and friction factor of TiO2 nanofluid flow in a tube with twisted tape inserts, Int. J. Therm. Sci. 81 (2014) 84–93.

[202] A. Azari, M. Derakhshandeh, An experimental comparison of convective heat transfer and friction factor of Al2O3 nanofluids in a tube with and without butterfly tube inserts, J. Taiwan Inst. Chem. Eng. 52 (2015) 31–39.

[203] M. Akhavan-Behabadi, M. Shahidi, M. Aligoodarz, An experimental study on heat transfer and pressure drop of MWCNT–water nano-fluid inside horizontal coiled wire inserted tube, Int. Commun. Heat Mass Transfer 63 (2015) 62–72.

[204] S.S. Chougule, S. Sahu, Heat transfer and friction characteristics of Al2O3/water and CNT/water nanofluids in transition flow using helical screw tape inserts–a comparative study, Chem. Eng. Process. 88 (2015) 78–88.

[205] M. Khoshvaght-Aliabadi, M. Eskandari, Influence of twist length variations on thermal–hydraulic specifications of twisted-tape inserts in presence of Cu–water nanofluid, Exp. Therm. Fluid Sci. 61 (2015) 230–240.

[206] L.S. Sundar, et al., Heat transfer and friction factor of multi-walled carbon nanotubes–Fe3O4 nanocomposite nanofluids flow in a tube with/without longitudinal strip inserts, Int. J. Heat Mass Transf. 100 (2016) 691–703.

[207] S. Chougule, et al., Heat transfer enhancements of low volume concentration CNT/water nanofluid and wire coil inserts in a circular tube, Energy Procedia 90 (2016) 552–558.

[208] R. Mashayekhi, et al., Application of a novel conical strip insert to improve the efficacy of water–Ag nanofluid for utilization in thermal systems: a two-phase simulation, Energy Convers. Manage. 151 (2017) 573–586.

[209] W. Bai, et al., Thermo-hydraulic performance investigation of heat pipe used annular heat exchanger with densely longitudinal fins, Appl. Therm. Eng. 211 (2022), 118451.

[210] M. Chandra Sekhara Reddy, V. Vasudeva Rao, Experimental investigation of heat transfer coefficient and friction factor of ethylene glycol water based TiO2 nanofluid in double pipe heat exchanger with and without helical coil inserts, Int. Commun. Heat Mass Transfer 50 (2014) 68–76.

[211] P.V.D. Prasad, A.V.S.S.K.S. Gupta, K. Deepak, Investigation of trapezoidal-cut twisted tape insert in a double pipe u-tube heat exchanger using Al2O3/water nanofluid, Procedia Mater. Sci. 10 (2015) 50–63.

[212] A. Karimi, et al., The effects of tape insert material on the flow and heat transfer in a nanofluid-based double tube heat exchanger: two-phase mixture model, Int. J. Mech. Sci. 156 (2019) 397–409.

[213] C. Gnanavel, R. Saravanan, M. Chandrasekaran, Heat transfer augmentation by nano-fluids and Spiral Spring insert in Double Tube Heat Exchanger–A numerical exploration, Mater. Today: Proc. 21 (2020) 857–861.

[214] M. Karuppasamy, et al., Numerical exploration of heat transfer in a heat exchanger tube with cone shape inserts and Al2O3 and CuO nanofluids, Mater. Today: Proc. 21 (2020) 940–947.

[215] S.K. Singh, J. Sarkar, Experimental hydrothermal characteristics of concentric tube heat exchanger with V-cut twisted tape turbulator using PCM dispersed mono/hybrid nanofluids, Exp. Heat Transfer (2020) 1–22.

[216] S.K. Singh, J. Sarkar, Thermohydraulic behavior of concentric tube heat exchanger inserted with conical wire coil using mono/hybrid nanofluids, Int. Commun. Heat Mass Transfer 122 (2021), 105134.

[217] M. Khoshvaght-Aliabadi, et al., Experimental assessment of different inserts inside straight tubes: nanofluid as working media, Chem. Eng. Process. 97 (2015) 1–11.

[218] P.D. Prasad, et al., Experimental study of heat transfer and friction factor of Al2O3 nanofluid in U-tube heat exchanger with helical tape inserts, Exp. Therm Fluid Sci. 62 (2015) 141–150.

[219] M. Khoshvaght-Aliabadi, M. Akbari, F. Hormozi, An empirical study on vortex-generator insert fitted in tubular heat exchangers with dilute Cu–water nanofluid flow, Chin. J. Chem. Eng. 24 (6) (2016) 728–736.

[220] P.D. Prasad, A. Gupta, Experimental investigation on enhancement of heat transfer using Al2O3/water nanofluid in a u-tube with twisted tape inserts, Int. Commun. Heat Mass Transfer 75 (2016) 154–161.

[221] S. Khanmohammadi, et al., Triple-objective optimization of a double-tube heat exchanger with elliptic cross section in the presence TiO 2 nanofluid, J. Therm. Anal. Calorim. 140 (1) (2020) 477–488.

[222] P.M. Kumar, M. Chandrasekar, Heat transfer and friction factor analysis of MWCNT nanofluids in double helically coiled tube heat exchanger, J. Therm. Anal. Calorim. (2020) 1–13.

[223] G. Huminic, A. Huminic, Heat transfer characteristics in double tube helical heat exchangers using nanofluids, Int. J. Heat Mass Transf. 54 (19–20) (2011) 4280–4287.

[224] Z. Wu, L. Wang, B. Sundén, Pressure drop and convective heat transfer of water and nanofluids in a double-pipe helical heat exchanger, Appl. Therm. Eng. 60 (1) (2013) 266–274.

[225] W.I.A. Aly, Numerical study on turbulent heat transfer and pressure drop of nanofluid in coiled tube-in-tube heat exchangers, Energy Convers. Manage. 79 (2014) 304–316.